Physical Geography
Publication details, including instructions for authors and subscription information:
http://www.tandfonline.com/loi/tphy20

Spatial persistence and temporal patterns in vegetation cover across Florida, 1982-2006

HuiPing Tsai[a], Jane Southworth[a] & Peter Waylen[a]
[a] Department of Geography, University of Florida, TUR 3414, P.O. Box 117315, Gainesville, FL 32611, USA
Published online: 04 Apr 2014.

Physical Geography, 2014
Vol. 35, No. 2, 151–180, http://dx.doi.org/10.1080/02723646.2014.898126

Spatial persistence and temporal patterns in vegetation cover across Florida, 1982–2006

HuiPing Tsai*, Jane Southworth and Peter Waylen

Department of Geography, University of Florida, TUR 3414, P.O. Box 117315, Gainesville, FL 32611, USA

(*Received 18 November 2013; accepted 4 February 2014*)

The study analyzes the spatial persistence and temporal patterns in vegetation cover across Florida by utilizing the Normalized Difference Vegetation Index (NDVI) time-series data derived from the Advanced Very High Resolution Radiometer from 1982 to 2006. Specifically, mean-variance analysis and persistence metrics are used to discern the significance of vegetation patterns, the significance of land cover and land-use change, and the relevance of climate variability across time and space. Results demonstrate a consistent, increasing pattern in the mean NDVI and its variance, especially during the late fall and winter season. A possible explanation of this increasing pattern is based on the Atlantic Multidecadal Oscillation, which switched from cold to warm phase after 1995 and is associated with increased winter precipitation. Additionally, the impacts of the El Niño Southern Oscillation can be detected through the decreased spatial variances of NDVI in warm-phase events, compared to cold-phase events, and the more pronounced nature of the pattern in fall/winter. This study proposes a novel set of techniques applied to satellite-derived vegetation data, which effectively discerns fine, statewide vegetation dynamics at appropriate spatial and temporal scales.

Keywords: NDVI; mean-variance analysis; spatial persistence analysis; climate variability; land-cover change

1. Introduction

The Earth's terrestrial surface is being transformed and altered by humans in unprecedented fashion in terms of pace, magnitude, and spatial reach (Lambin et al., 2001). Land use and land-cover change (LULCC) is the conversion and modification of the Earth's surface (DeFries, Field, Fung, Collatz, & Bounoua, 1999; Lambin & Ehrlich, 1996; Matthews, Weaver, Meissner, Gillett, & Eby, 2004; Turner et al., 1995) and its study is necessary for the maintenance of a healthy-functioning Earth (Baumann et al., 2011; de Chazal & Rounsevell, 2009; Drummond & Loveland, 2010; Eugenio, Richards, Walker, & Caldas, 2011; Feddema et al., 2005; Grimm et al., 2008; Lambin et al., 2001; Turner et al., 1995; Veldkamp & Lambin, 2001). An interdisciplinary framework referred to as Land Change Science (LCS) (Gutman et al., 2004; Lambin & Geist, 2006; Turner, Lambin, & Reenberg, 2007) utilizes environmental and human geography, and remote sensing/geographical information system (GIS) science to address questions concerning LULCC and the impacts of the changes on humankind and the environment, as an integrated science (Bounoua, DeFries, Collatz, Sellers, &

*Corresponding author. Email: htsai@ufl.edu

Khan, 2002; DeFries et al., 1999; Friedl et al., 2010; Gutman et al., 2004; Lambin et al., 2001; Rindfuss, Walsh, Turner, Fox, & Mishra, 2004; Shalaby & Tateishi, 2007; Southworth, Cumming, Marsik, & Binford, 2006; Turner et al., 2007; Xiao et al., 2006).

Vegetation performs valuable environmental functions: (1) conversion of the Sun's energy to forms usable by humans and other animals via photosynthesis (Allen et al., 1987; Choudhury, 1987; Gu et al., 2003; Running & Nemani, 1988), (2) provision of a major sink of carbon that would otherwise reside in the atmosphere, thereby regulating climate (Cao & Woodward, 1998; King, Post, & Wullschleger, 1997), (3) extraction of nitrogen as a step in transforming fairly inert atmospheric nitrogen to forms essential for growth (Bobbink, Hornung, & Roelofs, 1998; McGuire et al., 1992), and (4) transfer of water from subsurface stores to the atmosphere thereby maintaining precipitation and surface water flows (Bosch & Hewlett, 1982; Porporato, Laio, Ridolfi, & Rodriguez-Iturbe, 2001; Stephenson, 1990). The accelerating pace of LULCC in the past 50 years is of concern for biodiversity, climate regulation, and ecosystem services (DeFries, 2008; Foley et al., 2005) through its effects on net radiation, division of energy into sensible and latent heat, and partitioning of precipitation into soil water, evapotranspiration, and runoff (Foley et al., 2005) as evidenced by real-world examples (Bonan et al., 2002; Cuo, Lettenmaier, Alberti, & Richey, 2009; Feddema et al., 2005; Kalnay & Cai, 2003) and model simulations (Chase, Pielke, Kittel, Nemani, & Running, 2000; Marshall, Pielke, Steyaert, & Willard, 2004; Matthews et al., 2004; McAlpine et al., 2009; Wilson & Henderson-Sellers, 1985). A recent analysis suggests that anthropogenic impacts coupled with changes in seasonal and annual precipitation patterns can have dramatic widespread effects on ecosystem structure and function (Kaplan, 2012), but interactions between LULCC, climate variability, and vegetation dynamics are not easily explainable by any simple theory or model (National Research Council, 2005) and their representation remains a key challenge.

Remote sensing techniques furnish efficient tools with which to present a spatially and temporally consistent picture of land surface conditions (Bartholomé & Belward, 2005; Friedl et al., 2010; Gould, 2000; Lambin & Geist, 2006; Stow et al., 2004; Townshend, Justice, Li, Gurney, & McManus, 1991) and have been used increasingly in LCS to improve the observation and monitoring of land surface changes (Duncan, Shao, & Adrian, 2009; Gao, 1996; Gould, 2000; Tang, Li, & Tang, 2010; Townshend et al., 1991; Weng, 2002; Wu, Zhou, & Li, 2009; Zhou, Li, & Kurban, 2008). Major benefits of remote sensing are its ability to (1) collect standardized repeat measurements of the Earth's surface status and change (DeFries, 2008; Turner et al., 2003), (2) differentiate the character of environmental change, (3) determine the spatial location and spatio-temporal variation of environmental change, and (4) derive associations with potential driving variables (Southworth, Munroe, & Nagendra, 2004). Discrete and continuous remote sensing techniques are commonly applied in LCS research, both have advantages and limitations. The discrete approach, such as land-cover classification, requiring definition of precise classes based upon objective criteria (Di Gregorio & Jansen, 1998), is simple and clear but fails to quantify land surface heterogeneity adequately (Colditz, Schmidt, Conrad, Hansen, & Dech, 2011). The continuous approach applies original remotely sensed data or derived indices, such as a vegetation index, which can be directly linked to land surfaces processes (Southworth et al., 2004), but introduces issues such as spatial autocorrelation, leading to less clear-cut interpretations. An optimal method of analysis is one that minimizes the limitations of each while preserving their strengths, when using them in combination.

The Normalized Difference Vegetation Index (NDVI) is a commonly used continuous remotely sensed data product (Anyamba & Tucker, 2005; Fensholt & Proud, 2012; Gutman, 1999; Jacquin, Sheeren, & Lacombe, 2010; Lee, Yu, Price, Ellis, & Shi, 2002; Lu, Raupach, McVicar, & Barrett, 2003; Markon, Fleming, & Binnian, 1995; Pettorelli et al., 2005), which provides valuable information about plant phenology (de Jong, de Bruin, de Wit, Schaepman, & Dent, 2011; Jakubauskas, Legates, & Kastens, 2002; Lee et al., 2002; Lu et al., 2003; Martínez & Gilabert, 2009; Menzel, 2000; Sakamoto et al., 2005; Wang et al., 2004; Wardlow & Egbert, 2008), net primary productivity (Fuller, 1998; Hill & Donald, 2003; Ricotta, Avena, & De Palma, 1999), and the effects of LULCC (Immerzeel, Quiroz, & de Jong, 2005; Li, Kustas, Prueger, Neale, & Jackson, 2005; Scanlon, Albertson, Caylor, & Williams, 2002; Wessels, Prince, Frost, & van Zyl, 2004). Established time-series approaches are being adapted to address intra- and inter-annual variations in these sorts of Earth Observation data (Anyamba & Tucker, 2005; Eklundh & Olsson, 2003; Fensholt, Rasmussen, Nielsen, & Mbow, 2009; Helldén & Tottrup, 2008; Jeyaseelan, Roy, & Young, 2007; McCloy, Los, Lucht, & Højsgaard, 2005; Myneni, Keeling, Tucker, Asrar, & Nemani, 1997; Neeti et al., 2011; Olsson, Eklundh, & Ardö, 2005). The National Oceanic and Atmospheric Administration (NOAA) data-set of NDVI has been used for regional- to global- scale analysis of vegetation patterns (Anyamba & Tucker, 2005; Jeyaseelan et al., 2007; Olsson et al., 2005) and, given its relatively fine spatial resolution and lengthy (since 1981) temporal coverage, (Anyamba & Tucker, 2005; Fensholt et al., 2009; Myneni et al., 1997; Neeti et al., 2011), accords an excellent opportunity to employ time-series approaches to vegetation research.

Numerous methods have been developed to interpret NDVI time series, including functions fitted to time-series data (Jonsson & Eklundh, 2002), signal-noise discrimination (Millward, Piwowar, & Howarth, 2006), and the breaks for additive seasonal and trend method to detect seasonal and gradual changes within the time series (Verbesselt, Hyndman, Newnham, & Culvenor, 2010). Other techniques include principal components analysis (Anyamba & Eastman, 1996), fast Fourier transforms (Azzali & Menenti, 2000), change-vector analysis (Lambin & Strahlers, 1994), and harmonic analysis (Jakubauskas et al., 2002). However, many of these employ some form of transformation of the original time-series data and present challenges in labeling and identifying change components (Verbesselt et al., 2010). Waylen, Southworth, Gibbes, and Tsai (in press) propose some simple statistical tests to determine the significance of land-cover changes reflected in three separate persistence metrics designed to distinguish landscape changes on a pixel-by-pixel basis. These metrics are designed to capture the direction (increase/decrease) and magnitude of change in NDVI, taking into account seasonal changes and the gradual and abrupt changes likely in ecosystems (Verbesselt et al., 2010), to identify areas of climatically or anthropogenically induced alterations. This research applies this methodology to a time series of NDVI from 1982 to 2006, along with mean-variance analysis (Pickup & Foran, 1987), to identify seasonal and inter-annual variability in vegetation dynamics and the significance of LULCC in Florida. These methods allow for a characterization of vegetation dynamics and the relevance of LULCC in a spatially explicit manner, while also providing a picture of NDVI seasonality and its response to climate and disturbance (Washington-Allen, Ramsey, West, & Norton, 2008; Washington-Allen, West, & Ramsey, 2003; Zimmermann et al., 2007).

Vegetation structure and pattern has been studied intensively in several regions such as Everglades National Park (Gaiser, McCormick, Hagerthey, & Gottlieb, 2011; Huang, Saiers, Harvey, Noe, & Mylon, 2008; Todd et al., 2010), South Florida (LaRoche &

Ferriter, 1992; Menges & Deyrup, 2001; Ross, Ruiz, Sah, & Hanan, 2009), and in specific ecosystems (Haile, Nair, & Nair, 2010; Harley, Grissino-Mayer, & Horn, 2012; Sitch et al., 2003; Smith & Pain, 2009). However, there is no comprehensive, statewide, overview of patterns of vegetation and change. An evaluation of spatial and temporal patterns of vegetation cover, and change statewide is required to establish benchmarks and enhance understanding of long-term environmental changes. Specific research questions addressed are: (1) What are the patterns of LULCC across Florida between 1981 and 2006? (2) How do these patterns vary with season, climate zone, and LULCC class? and (3) Do persistence analyses and associated tests contribute meaningfully to this understanding and to studies of future vegetation dynamics?

2. Study area

The population of Florida (Figure 1) increased by over 16 million between 1940 and 2010 (US Census Bureau, 2012), so that the state currently supports a population density of over 135/km^2 on its 138,887 km^2 area. These changes, in combination with climate variability, have led to direct and indirect impacts on LULCC and vegetation

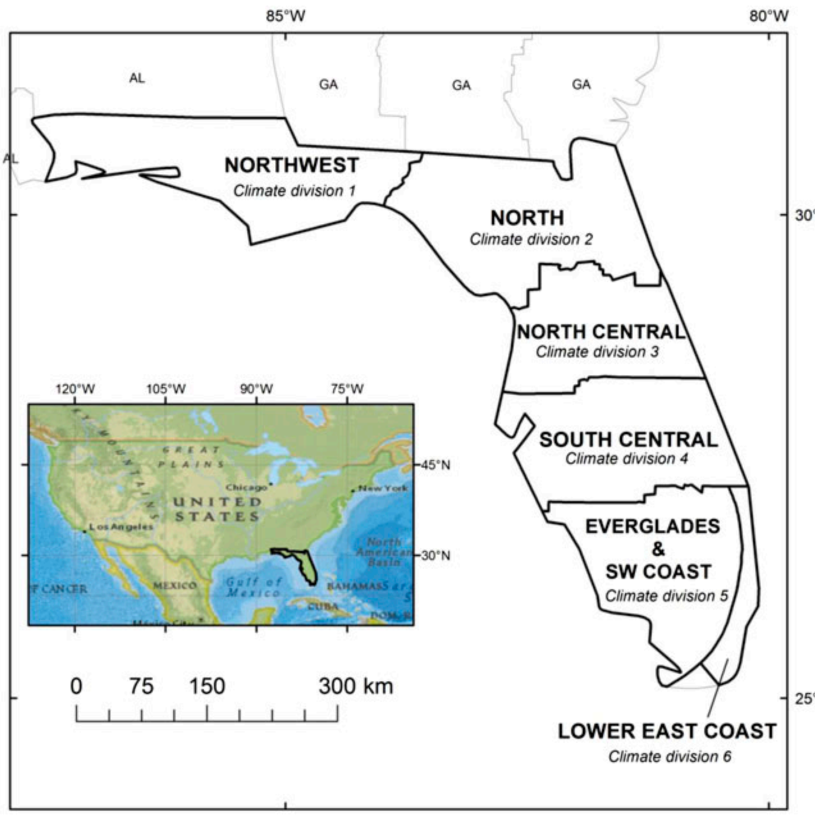

Figure 1. The six climate divisions of Florida employed in the study. Throughout the text, the Northwest division is referred to as climate division 1, North as climate division 2, North Central as division 3, South Central as division 4, Everglades and SW Coast as division 5, and Lower East Coast as division 6.

dynamics, transformed by agriculture, urbanization, and the diversion of surface water features (Marshall et al., 2004).

Dominant drivers of Florida's climate include latitude, land and water distribution, prevailing winds, storms, pressure systems, and ocean currents. Most of the state lies within the southerly extreme of the humid subtropical climate zone, noted for its long hot, humid summers and mild, wet winters. Southernmost parts of the state are generally designated as tropical savanna, or wet and dry tropics (Henry, Portier, & Coyne, 1994). Annual precipitation averages approximately 1350 mm with the panhandle and southeast being wettest, and the Florida Keys and Cape Canaveral area, the driest. The panhandle and north receive winter frontal and summer convective rains, with frontal influence declining southward (Henry et al., 1994; Jordan, 1984). Position and intensity of the Azores-Bermuda High Pressure system exerts a powerful influence on peninsular Florida's weather during the winter. Summer rainfall commences in the southeast in late April and moves northward, while the fall dry season begins in the north in late September and spreads south, arriving in south Florida in mid-November. Tropical storms can play an important role in the summer rainfall and may postpone the arrival of the dry season. On average, the North Atlantic hurricane season peaks in August/September, and the extensive coastline makes the state prone to impacts of land-falling tropical systems.

Large-scale, low-frequency causes of climate variability should be considered in such a time-series-based study. The regional relationship with El Niño Southern Oscillation (ENSO) has been studied extensively (Abtew & Trimble, 2010; Gischler, Hudson, & Storz, 2009; Hansen, Hodges, & Jones, 1998; Jagtap et al., 2002; Misra & DiNapoli, 2012; Schmidt, Lipp, Rose, & Luther, 2001; Schmidt & Luther, 2002). Although seated in the equatorial Pacific, ENSO causes shifts in the position of the sub-tropical and polar jet streams that steer frontal systems across North America. During warm phases of ENSO (El Niño), Florida typically experiences 30–40% more winter rainfall and cooler temperatures, while cold phases (La Niña) bring warmer, drier winters and springs, which frequently trigger drought and wildfires (Harrison, 2013). The exact nature and timing of the changes vary across the state.

NOAA divides Florida into seven climate divisions, which are generally considered to constitute climatically homogeneous regions (Keim, Fischer, & Wilson, 2005) (Figure 1). Six are examined in this research, with the Florida Keys (division VII) excluded due to its distinct local climate and limited surface area relative to the resolution of the remote sensing data.

3. Methods

3.1. NDVI vegetation cover data

Analyses of seasonal and inter-annual vegetation dynamics and patterns are based on the NDVI data derived from sensors aboard the NOAA polar-orbiting satellite series (NOAA-7, 9, 11, 14, 16, and 17). The vegetation index is a function of radiation absorbed by chlorophyll in the red band and scattering by cellulose in the near infrared, and is a variant of the simple ratio of the near-infrared and red bands defined as:

$$\mathrm{NDVI} = \frac{\text{Near Infrared} - \text{Red}}{\text{Near Infrared} + \text{Red}}. \tag{1}$$

By computing the ratio as the difference of the two wavelengths over the sum of the two wavelengths, NDVI is normalized, so that the range falls between −1 and +1. High values (closer to +1) indicate abundant healthy green vegetation and values near or below zero indicate an absence of vegetation (Warner & Campagna, 2009). The index is widely accepted as an indicator of vegetation properties and used to assess ecological response to environmental changes over broad geographic regions (Anyamba & Eastman, 1996; Barbosa, Huete, & Baethgen, 2006; Bégué, Vintrou, Ruelland, Claden, & Dessay, 2011; Carlson & Ripley, 1997; Gurgel & Ferreira, 2003; Jarlan, Tourre, Mougin, Philippon, & Mazzega, 2005; Li & Kafatos, 2000; Meng, Ni, & Zong, 2011; Pettorelli et al., 2005; Philippon, Jarlan, Martiny, Camberlin, & Mougin, 2007).

The Advanced Very High Resolution Radiometer GIMMS NDVI data-set, from July 1981 to December 2006, has been used for numerous regional- to global-scale vegetation studies (Anyamba & Tucker, 2005; Fensholt et al., 2009; Hogda, Karlsen, & Solheim, 2001; Los, Justice, & Tucker, 1994; Milesi et al., 2010; Raynolds, Walker, Epstein, Pinzon, & Tucker, 2012; Tucker et al., 2005; White & Nemani, 2006), and has been corrected for numerous potential errors such as residual sensor degradation and sensor inter-calibration differences. The spatial resolution is 8 km and the data record is based on 15-day composites of the maximum-recorded NDVI to construct cloud-free views of the Earth. The state boundary covering the domain 25–30°N, 79–87°W is subset from the data-set for the period January 1982–December 2006. Since the data-set was constructed based on 15-day maximum composites, two such composites occur each month. For this study, the higher value composite is chosen to represent the value for the month.

3.2. NOAA CCAP land-cover classification data

Florida land-cover classification data are available from the Coastal Change Analysis Program (C-CAP) developed by NOAA in collaboration with the Department of Commerce, National Ocean Service and NOAA Coastal Services Center. Current production of the C-CAP land-cover data-sets is accomplished through closely coordinated efforts with the United States Geological Survey, which produces the National Land Cover Data-set. Since C-CAP data are developed primarily from Landsat Thematic Mapper satellite imagery, the spatial resolution is 30-m pixels on the ground. Current C-CAP data-sets are available for Florida in the years 1996, 2001, and 2006 for land cover and land use across 23 classes. To simplify for the following analyses, the classes were regrouped into 10 broader classes (Table 1). These classes are: (1) developed land, (2) agricultural land, (3) grassland, (4) forested land, (5) scrub land, (6) palustrine wetlands, (7) estuarine wetlands, (8) barren land-unconsolidated shore, (9) barren land, and (10) water and submerged lands. Pixels remaining in the same land-cover class on all three observation dates are extracted for later use as a control data-set.

3.3. Mean-variance analysis

Mean-variance analysis (Pickup & Foran, 1987) characterizes the spatiotemporal behavior of remotely sensed vegetation indices and has been used to describe seasonal and inter-annual responses of vegetation to climate and disturbance in several regions (Washington-Allen et al., 2008, 2003; Zimmermann et al., 2007). The mean can be interpreted as indicating the overall amount of vegetation within the landscape and the variance as the degree of landscape heterogeneity.

Table 1. CCAP land-cover classes and regrouped classes employed in this study with their land areas (%) in Florida.

Original class	Regrouped class	Land area (%) 1996	2001	2006
Developed high intensity	Developed land	9.50	10.40	10.60
Developed medium intensity				
Developed low intensity				
Developed open space				
Cultivated crops	Agricultural land	17.50	17.30	17.10
Hay/pasture				
Grassland/herbaceous	Grassland	3.50	3.50	3.90
Deciduous forest	Forest land	18.00	17.50	16.20
Evergreen forest				
Mixed forest				
Scrub/shrub	Scrub land	7.80	7.70	8.50
Bare land	Barren land	0.40	0.50	0.70
Palustrine forested wetland	Palustrine wetlands	36.1	36.0	35.8
Palustrine scrub/shrub wetland				
Palustrine emergent wetland				
Estuarine forested wetland	Estuarine wetlands	3.10	3.10	3.10
Estuarine scrub/shrub wetland				
Estuarine emergent wetland				
Unconsolidated shore	Unconsolidated shore	0.03	0.03	0.03
Open water	Water and submerged lands	3.90	3.90	4.00
Palustrine aquatic bed				
Estuarine aquatic bed				

Figure 2 depicts hypothetical relationships between mean-variance and vegetation status (Washington-Allen et al., 2008). Each quadrant demonstrates differing degrees of heterogeneity (variance) and vegetation status (mean). Exact interpretations depend on the type of landscape and research design. Broadly, Quadrant 1 (low mean and variance) represents the most degraded landscape, with homogeneously low amounts of vegetation. Quadrant 2 (low mean and high variance) suggests that a high proportion of the landscape tends towards bare ground and is thus susceptible to disturbance. Quadrant 3 (high mean and low variance) implies greater, homogeneous vegetation cover, and Quadrant 4 (high mean and variance) indicates the landscape possesses both higher vegetation cover and a higher spatial variability. The "ideal" quadrant depends on the dominant land-cover classes. For example, climate divisions 1 and 2 have large proportions of forest, for which the ideal quadrant could be Quadrant 3 (high mean and low variance). The approach permits the description of the trajectory of vegetation across the 25-year time period in terms of both its mean and variance. In addition to the monthly data, patterns are examined at two temporal scales: annual (cumulative monthly NDVI from January to December), and seasonal for fall/winter (accumulation over October–March) and spring/summer (April–September).

3.4. Persistence metrics

Three persistence metrics are adopted from Waylen et al. (in press). Directional and relative directional persistence are designed to capture the direction of increase/decreases in NDVI, and massive persistence measures the magnitude of changes. It is assumed

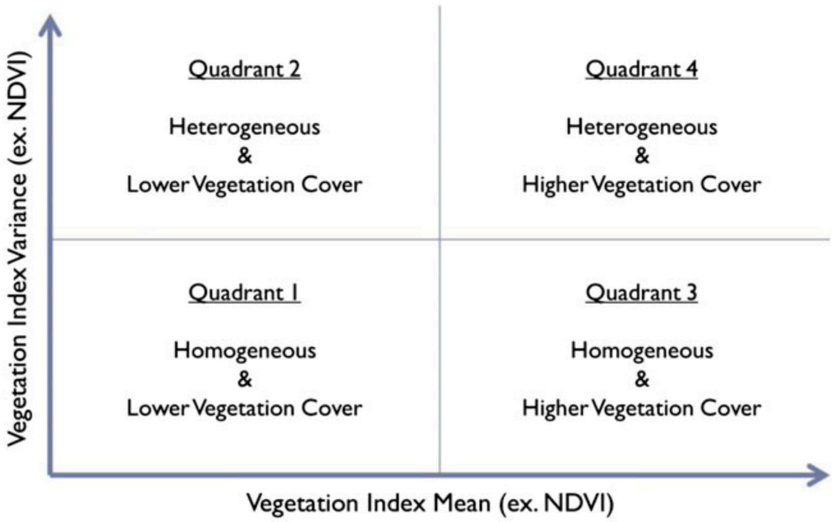

Figure 2. Hypothetical relationship between mean-variance of a vegetation and vegetation status [adapted from Washington-Allen et al. (2008)]. The *X*-axis represents the mean of a specific vegetation index while the *Y*-axis represents the variance over space. Each quadrant indicates the status of a landscape.

that without any disturbances to surface vegetation (e.g., LULCC, climate variability, land-cover modification), values of NDVI are normally distributed and serially independent (i.e., independent from one year, season, or month to the next, e.g., January 1982 and January 1983). Based on the null hypothesis, statistical significance levels of all three metrics can be established in order to highlight areas that have experienced unusual changes.

3.4.1. *Directional persistence*

This metric, D, captures the cumulative directional change over the time series relative to the first observation and is determined as follows:

$$D_j = \sum_{i=2}^{n} t_{i,j} \tag{2}$$

$$V_{1,j} < V_{i,j} : \ t_{i,j} = +1$$

$$V_{1,j} > V_{i,j} : \ t_{i,j} = -1$$

where $V_{i,j}$ is the monthly value of NDVI, in year i, month j. A value +1 is assigned, if a pixel records a value of NDVI greater than the base observation; and −1 is assigned if less. However, the directional persistence measure should be interpreted with care as it is a function of the base year selected for the analysis, which must be either (1) a scientifically valid selection based on criteria or set rationale, such as investigating the impact of an event on a landscape, like recovery time post drought, or (2) verifiably "typical" e.g., not a flood year or drought year, as this would significantly impact the results. In this application, values at the start of this series may reflect impacts of the shift in global circulation in the late 1970s (Deser, Phillips, & Hurrell, 2004), and the base year, 1981, is fairly "typical" in terms of precipitation climate, classified as a neutral ENSO year (COAPS, 2014).

3.4.2. *Relative directional persistence*

The metric, R, makes directional comparisons relative to the observation in the preceding year rather than a base value, for example the observation in May 1988 is compared to that of May 1987, and therefore reflects sequential cumulative directional change:

$$R_j = \sum_{i=2}^{n} t_{i,j} \tag{3}$$

$$V_{i,j} < V_{i+1,j} : \ t_{i,j} = +1$$

$$V_{i,j} > V_{i+1,j} : \ t_{i,j} = -1$$

and is free of some of the restrictive assumptions concerning the base value which might influence D. The two measures provide valuable, complementary landscape-scale measures.

3.4.3. *Massive persistence*

The prior measures only account for the direction of change and not its magnitude and are therefore insensitive to abrupt "step" changes in a series as opposed to more monotonic changes. The massive persistence variable, M, also incorporates the magnitude:

$$M_j = \sum_{i=2}^{n} \left(V_{i+1,j} - V_{i,j}\right) \tag{4}$$

However, it introduces new statistical challenges as the variance of NDVI needs to be considered when computing statistical significance (the other two reduced to standard normal distributions). Thus, the metric can only be evaluated for a particular type of LULCC, at a set time of year, and for a particular climate division, all of which could impact the variance, and therefore magnitudes, of sequential steps. As such, it is not transferable across regions and needs ancillary data for its use.

The original GIMMS data are scaled from −1000 to +1000 and therefore truncate values of NDVI to three decimal places. Theoretically, the probability of identical sequential values of NDVI is zero; however, formated in this way, they can occur, resulting in zero change in the two directional metrics. To resolve a direction of change for the 1.09% of occasions when this is an issue, a GIS technique is employed to assign a value based on the majority of values from the surrounding 5 by 5 window of pixels.

4. Results

4.1. Mean-variance analysis

Both mean annual NDVI and its spatial variance (Figure 3) exhibit slight increases from the 1980s to 2000s. In the 1980s, annual values were highly variable, covering all four quadrants, although the lowest mean NDVI is found in 1982. The dominant

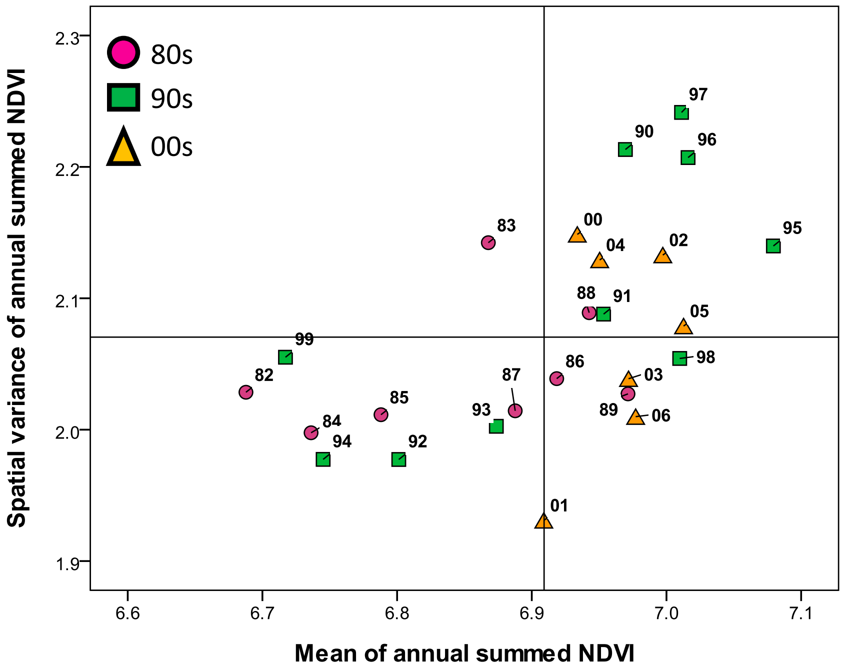

Figure 3. Mean-Variance plot for annual summed NDVI throughout Florida. The *X*-axis represents the mean of annual summed NDVI and the *Y*-axis represents the spatial variance of the annual summed NDVI. The overall mean and variance for the time period are marked by black lines. Labels reference the year (e.g., 92 = 1992), and are color coded by decade (color figures are available in the online version of this article). 1980s in purple circles, 1990s in green squares, and 2000s in orange triangles.

pattern of vegetation cover in the decade however, is one of low variance and low to high mean, with means increasing in the later years. The early 1990s continued this pattern up through 1992–1994, when the values revert to lower mean and variance. Post-1994, increases in mean and variance are amongst the highest – reflecting significant growth rates and high variability across the state. High values of the mean are maintained in the 2000s and variance is moderate to high, especially later in the decade. The increase in both mean and variance across the state is marked (Figure 3). A similar pattern emerges in the winter data (Figure 4(a)); however, summer NDVI evinces no clear pattern (Figure 4(b)). As would be expected, mean values are generally higher during summer and lower in winter, but winters show increase after 1995 that are not present in summers. No discernible patterns emerge from mean-variance analysis of monthly data, suggesting that it is too fine a scale to detect such long-term changes.

4.2. *Persistence metrics*

All three persistence metrics assume that NDVI is normally distributed. Given that the index is bounded, and tends to become “saturated” at high values, there is cause to question this assumption. Time series of pixels corresponding to locations that remained unchanged in their CCAP classification (show no signs of LULC change) are extracted and compared to a fitted normal distribution. In over 85% of the cases, there is

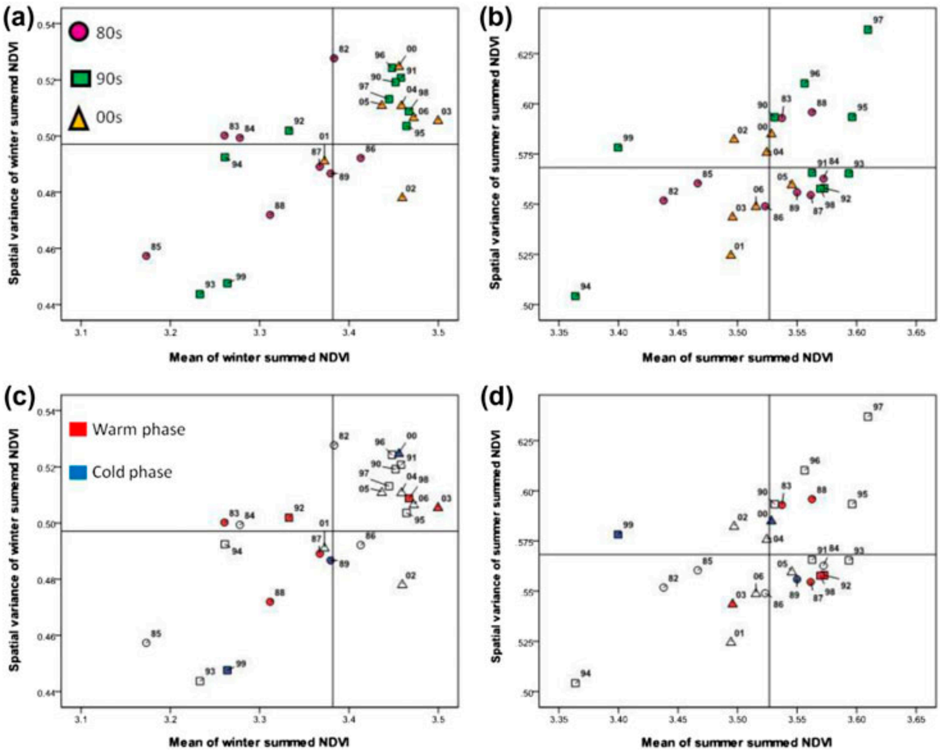

Figure 4. Mean-Variance plots for (a) winter NDVI and (b) Summer NDVI. Color coded by decade as in Figure 3, and (c) Winter NDVI and (d) Summer NDVI color coded for phase of ENSO (warm phase in red and cold phase in blue). The *X*-axis represents the mean of winter/summer summed NDVI and the *Y*-axis represents the spatial variance of the winter/summer summed NDVI. Labels reference the year (e.g., 92 = 1992), and (a) and (b) are color coded by decade. 1980s in purple circles, 1990s in green squares, and 2000s in orange triangles.

insufficient evidence to reject the null hypothesis of no significant difference between the observed distribution and fitted normal.

4.2.1. Directional persistence

This metric resembles the classic random walk process (Wilson & Kirkby, 1980), in which the probability of a success (positive step) is defined by the probability of exceeding the initial or base value. Critical scores can be determined by taking the inverse of the binomial distribution for a probability equivalent to the desired significance level. All subsequent significance levels are $\alpha = 0.05$ unless otherwise stated.

Figure 5 depicts values of directional persistence using 1982 as the base year. In general, positive scores prevail although some large negative values are evident from February to April and August to September. In February, these are concentrated in central to south Florida, becoming particularly pronounced further north during March and, to a lesser degree, April. In August, the central panhandle and coastal areas display pronounced negative scores, shifting to the northeast coast, central, and south Florida in September. October and November are months in which most of Florida returns positive scores.

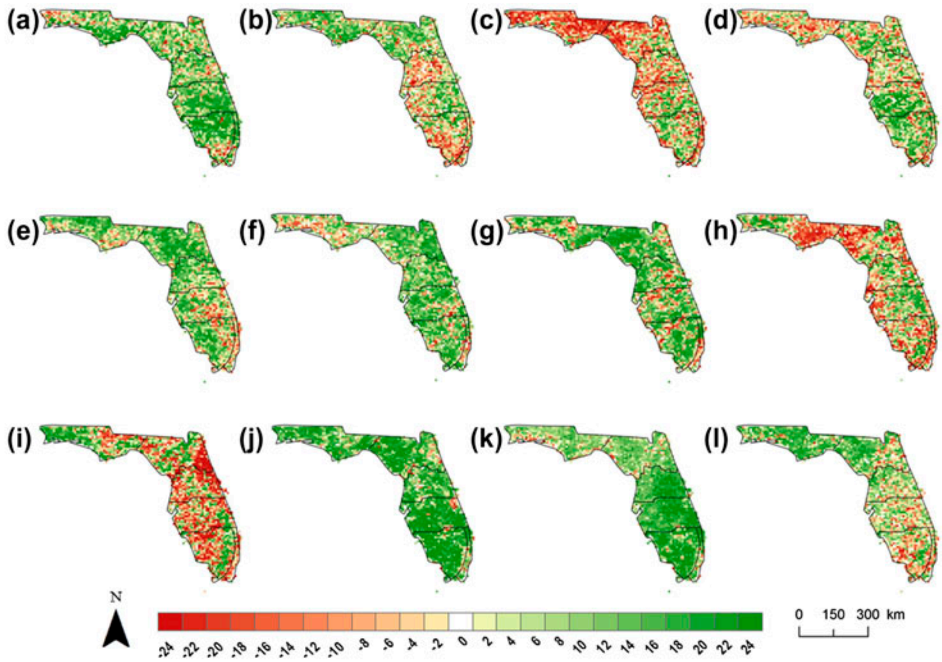

Figure 5. Values of directional persistence metric, D, for (a) January to (l) December 1982–2006. Directional persistence variable is calculated based on comparisons of NDVI observation in a month to the observation in the same some in the base year (this study uses 1982 as the base year). Positive scores (greening) are shown in hues of green and negative scores (declining greenness) are in red.

The northwest and north divisions show persistent positive scores from October to February, a pattern of negatives from March to April and August to September, and mixed patterns from May to July. Both central Florida divisions exhibit negative scores in latewinter/ early spring (February and March) and late summer/early fall (August and September), and a mixture in December. The Everglades and SW coast shows noticeable negative scores in February, August, September, and December, while the southeast records declining scores in March, August, and September and mixed patterns in February, May–July, and December.

Figure 6 identifies only those pixels returning statistically significant scores. Increasing scores overwhelmingly occur across the state in most months (January, May–July, October–December). Declines are still apparent in March, August, and September, and more weakly so in February and April. Northwest and north divisions experience secondary peaks in precipitation during winter (November–March) of about half the size of those in summer. According to the recent national climate assessment for the southeast region of the United States (USGCRP, 2009), average fall precipitation has increased by 30% since the 1900s, and Florida has experienced a noticeable increase in winter precipitation. The pronounced pattern of significant positive scores found in these two divisions from October to February is in keeping with these observations.

When directional persistence is considered for specific land covers, it is not surprising that significant negative scores are found in areas of developed land in almost all months, reflecting the increased presence and density of urbanization (Figure 7). Another prominent regional feature warranting further investigation is the negative

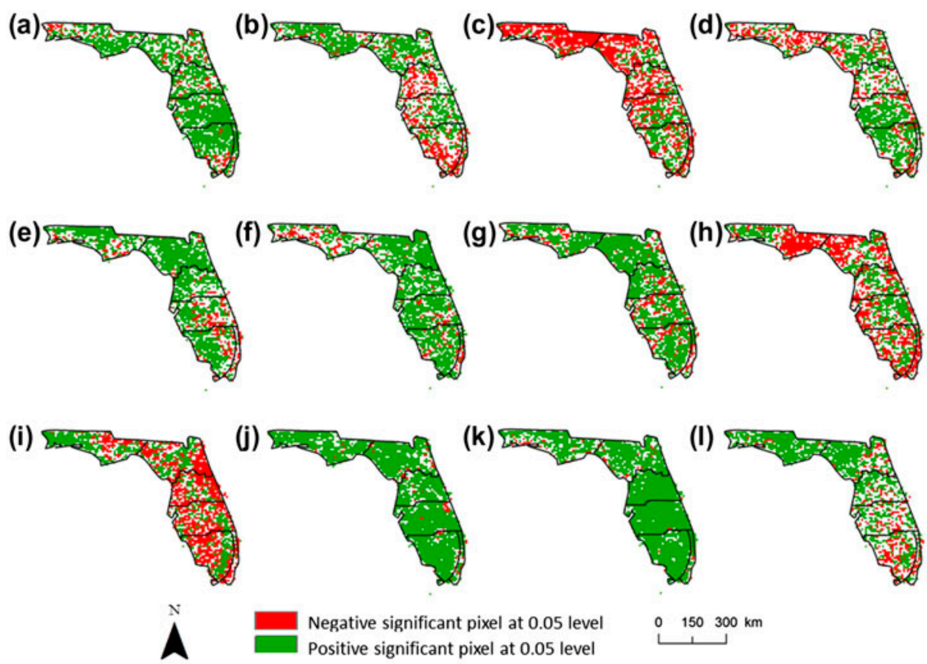

Figure 6. The statistically significant pixels at 0.05 level for directional persistence metric, *D*, from (a) January to (l) December 1982–2006. Positive significant scores are shown in green and negative significant score in red.

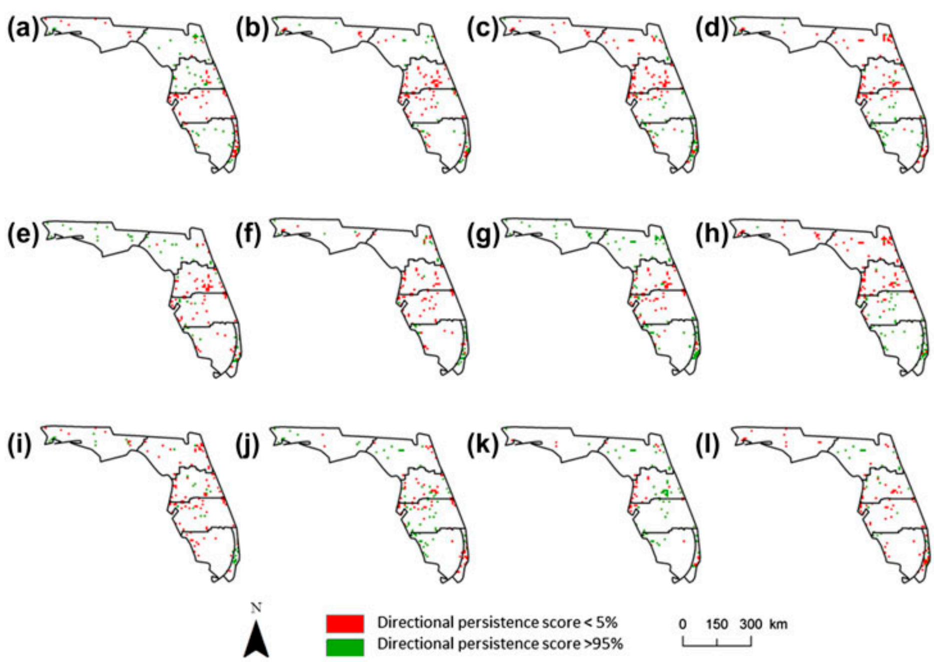

Figure 7. The statistically significant pixels at 0.05 level for directional persistence variable, *D*, for developed land only from (a) January to (l) December 1982–2006. Positive significant scores are shown in green and negative significant scores in red.

scores in agricultural lands at the southern part of Lake Okeechobee in climate division 5 (Figure 8). Palustrine wetlands (Figure 9) also elicit strong significant declines through much of the state, indicating a loss of wetland habitat.

4.2.2. Relative directional persistence

The less-pronounced patterns in these scores (Figure 10) might be expected, given the sensitivity of the metric to the presence/absence of sequences of continuously increasing or decreasing values of NDVI, as opposed to comparison to the first observation. The northwest dominantly returns positive values from September to February, except for December. North Florida displays a mixed pattern in almost all months; however, December, January, March, April, and August all show more negative scores than others. Central Florida divisions exhibit positive scores from October to February, again except for December; other months offer a mixed pattern. Southwest and southeast divisions present a similarly mixed pattern for all the months; however, their most southerly portions return large negative patterns in January and February. Similar regional and temporal patterns are evident in maps (Figure 11) of pixels returning statistically significant scores.

Figure 12 plots the cumulative frequency of relative persistence scores and those that would be expected of a stationary standard normal distribution. March and May indicate statewide behavior conformal with the assumption of a stationary Gaussian process. The degree of curvature of the function away from the 1:1 diagonal is indicative of difference from the hypothesized condition. Curvature above the diagonal

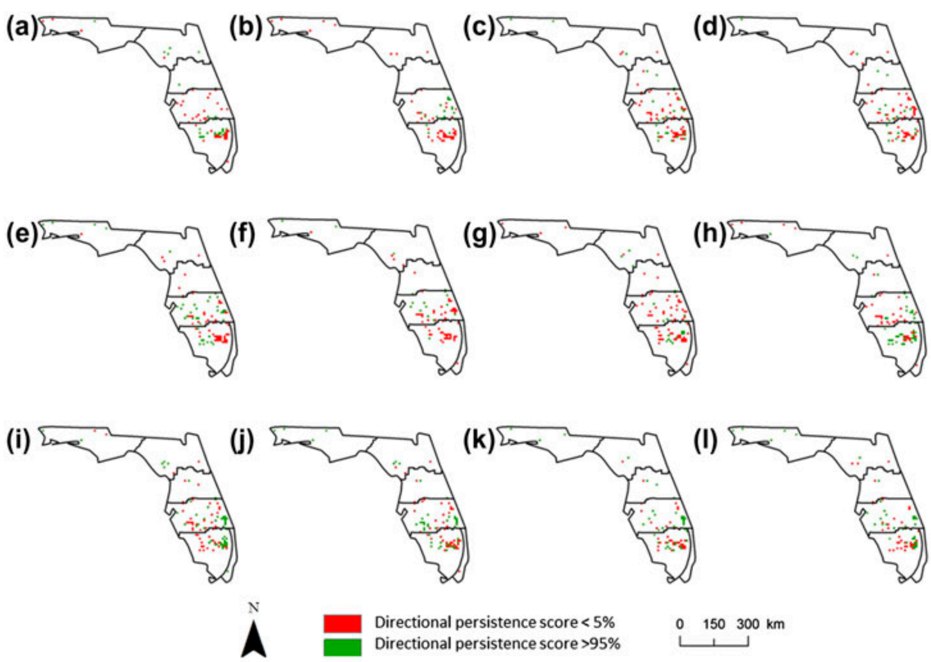

Figure 8. The statistically significant pixels at 0.05 level for directional persistence variable, *D*, for agricultural land only from (a) January to (l) December 1982–2006. Positive significant scores are shown in green and negative significant scores in red.

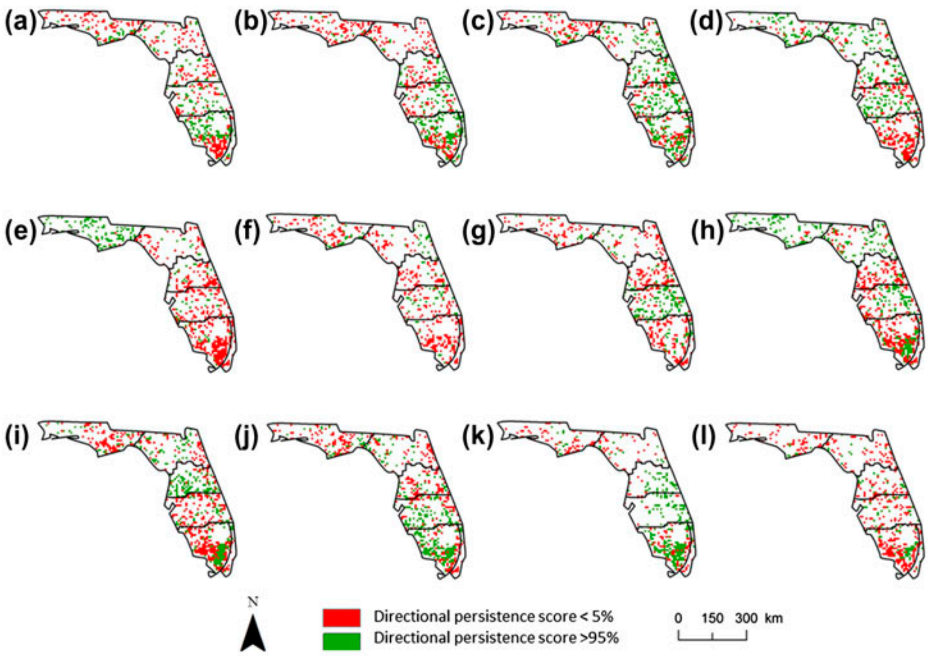

Figure 9. The statistically significant pixels at 0.05 level for directional persistence variable, *D*, for palustrine wetland only from (a) January to (l) December 1982–2006. Positive significant scores are shown in green and negative significant scores in red.

implies a greater frequency of negative scores and curvature below implies greater positive scores. November elicits the greatest curvature (positive scores) from the null condition. Other months suggesting a preponderance of positive scores include January, February, July, September, and October. April, June, August, and December all convey slightly more sequences of declining NDVI values.

4.2.3. Massive persistence

The massive persistence metric (Figure 13) suggests a statewide positive pattern in greenness in October and November. In the northwest and north, these give way to negative values from December through to April, peaking in March. August also exhibits negative scores for these divisions with coastal areas showing stronger negative values from May to July and also in September. Central divisions demonstrate an opposite signal in January; the northern region being slightly negative while the southern has a strong positive signal particularly in February. During other months, the central divisions display a mixed pattern. May and September seem to have stronger negative signals. Southwest and southeast divisions return high positive scores in January; however, the coastal areas and the extreme southern part appear to have negative scores.

According to the theoretical development, changes within specific land-cover classes and climate zone can be evaluated, where the C-CAP yields many pixels whose classification has remained unchanged. These pixels constitute “controls” describing the “typical” distribution of NDVI in a particular land cover, climate zone, and month.

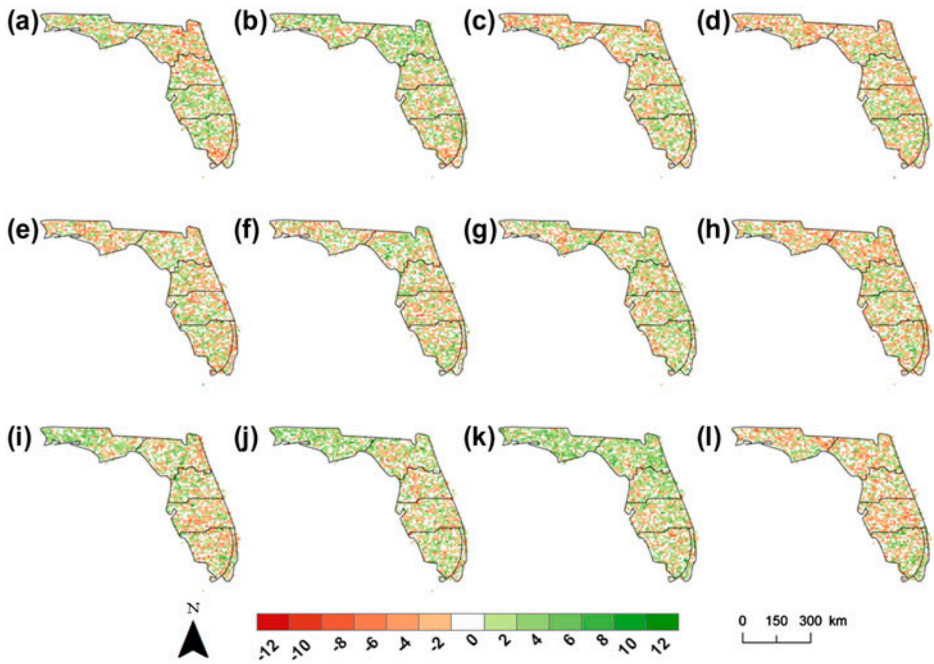

Figure 10. Relative directional persistence metric, *R*, from (a) January to (l) December 1982–2006. Relative directional persistence, *R*, is calculated based on comparisons of NDVI observation to the same month from the preceding year. Positive scores are shown in green and negative scores in red.

Only three land-cover classes of the 10 – developed land, agricultural land, and palustrine wetlands – yield sufficiently large numbers of pixels to permit significance testing of the *M* scores.

Monthly maps (Figure 14) display the percentage of pixels returning significant values of the metric (positive and negative) in each land-cover category and climate division. For developed land, significant positive changes dominate all climate divisions from October to February. Negative values become more common from March onward, especially in the southeast. The preponderance of negative values increases in March through May. June, September, and December indicate approximately the 5% of pixels returning significant values as might be expected at random. During July and particularly August, the high percentage of negative values of pixels in the southeast is clear. October and November are months during which positive values prevail across Florida.

High positive values returned by agricultural land (Figure 15), in January, February, October, and November, occur statewide. The only unusually frequent occurrences of pixels with negative scores are restricted to March in the south, spreading to central areas in April and May. Positive values concentrated in the south during July give way to negative ones in August and September. Similar temporal and spatial patterns are observed in the proportions of palustrine wetland pixels (Figure 16). Winter months generally return a high proportion of pixels with larger values of the metric. As observed in other land covers, patterns in December are less marked. During spring, negative values spread from the south (March) northward to central Florida in April

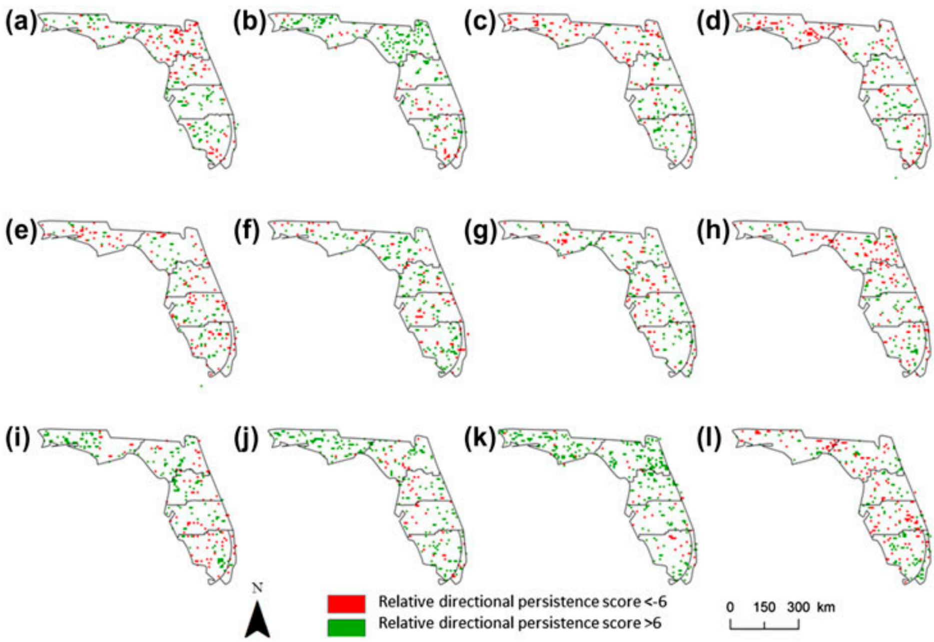

Figure 11. Pixels returning statistically significant (0.05 level) values of the relative directional persistence metric, R, from (a) January to (l) December 1982–2006. Positive significant scores larger than +6 are shown in green and negative significant scores of less than −6 in red.

and May. June is again marked by an absence of significant values, while July elicits more positive values and August shows a greater prevalence of significant negative values.

5. Discussion

This study demonstrates a new approach combining mean-variance analysis with a set of spatial persistence metrics and tests to derive indications of LULCC from a remotely sensed vegetation index time series. Individually, each metric has its own strengths and weaknesses, but, taken collectively, common spatio-temporal patterns emerge from the wealth of data. At the level of climate divisions, any such patterns are most likely related to climate variability/change – particularly precipitation – over the period of the satellite record. Anomalous or singular behavior of individual pixels or groups of pixels within a division is more likely to reflect localized LULCC. Table 2 provides a summary of the results, combining results for individual months and climate divisions, using each of the three metrics to summarize possible seasonal and regional changes at the climate-division level.

Changes in winter season patterns seem to dominate this landscape. Impacts of ENSO during winter months can be seen in the mean-variance analysis (Figure 4), where warm phases elicit higher mean NDVI than cold phases. Spatial variances are also lower in the warm phase, most markedly so in the fall/winter. These results correspond to extensively documented impacts of ENSO on regional precipitation (Beckage, Platt, Slocum, & Panko, 2003; Cronin, 2002; Enfield, Mestas-Nuñez, & Trimble, 2001;

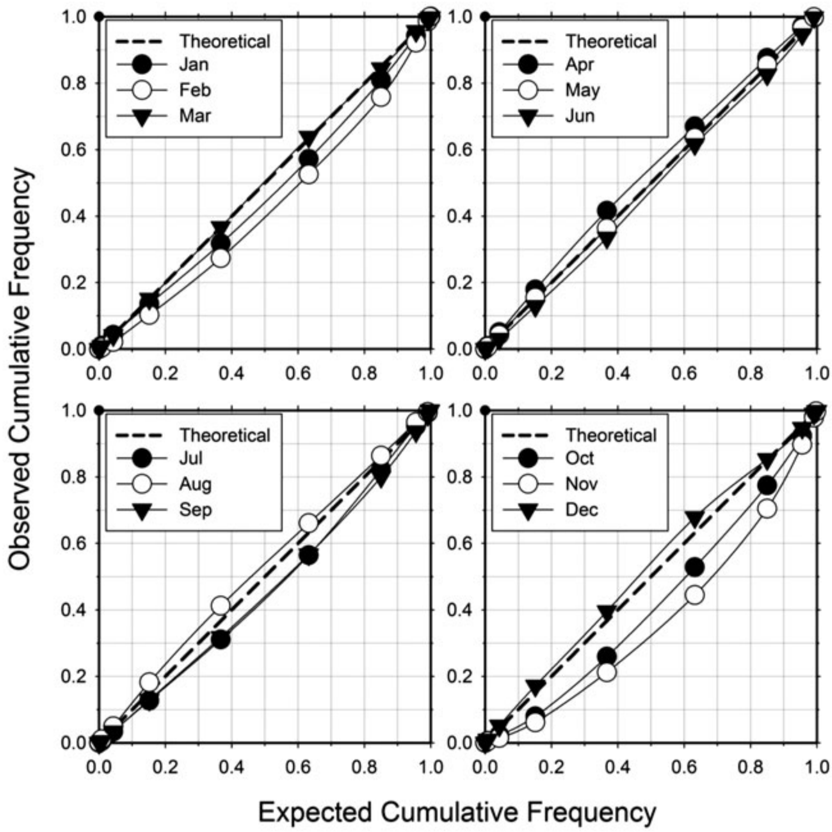

Figure 12. Cumulative frequency plots comparing observed monthly values of the relative direction persistence metric, *R*, with simulated normal distribution for each month. Points represent the discrete classes of scores that *R* could assume as indicated in the legend to Figure 10.

Gershunov, 1998; Jagtap et al., 2002; Ropelewski & Halpert, 1986; Schmidt et al., 2001; Schmidt & Luther, 2002; Vedwan et al., 2008; Wu, Hsieh, & Shabbar, 2005; Zorn & Waylen, 1997). The switch in ENSO phase from warm (1997–1998) to cold (1998–1999) and associated alternation in regional winter precipitation may provide one explanation for the 1999 outlier in the mean variance analysis, as warm phases typically bring wetter and cooler fall/winter conditions. Figure 4(c) indicates a more stable pattern of variance and mean during winters in warm phase years than cold in accordance with the presence of a less water-limited environment. The pronounced seasonality of precipitation and its dependence upon ENSO has tremendous consequences for water-resources planning and regional operations (Obeysekera, Irizarry, Park, Barnes, & Dessalegne, 2011), and might be expected to impact NDVI through agricultural yields (Hansen, Jones, Kiker, & Hodges, 1999), salinity (Cronin, 2002; Schmidt & Luther, 2002), and severe wildfires (Brenner, 1991; Brolley, O'Brien, Schoof, & Zierden, 2007; Harrison, 2013).

At the seasonal scale, results from the mean-variance and persistence analyses reveal increasing NDVI and spatial variance, especially in the late fall/winter, most notably in October and November, and less so in December. Spring (March–May) and

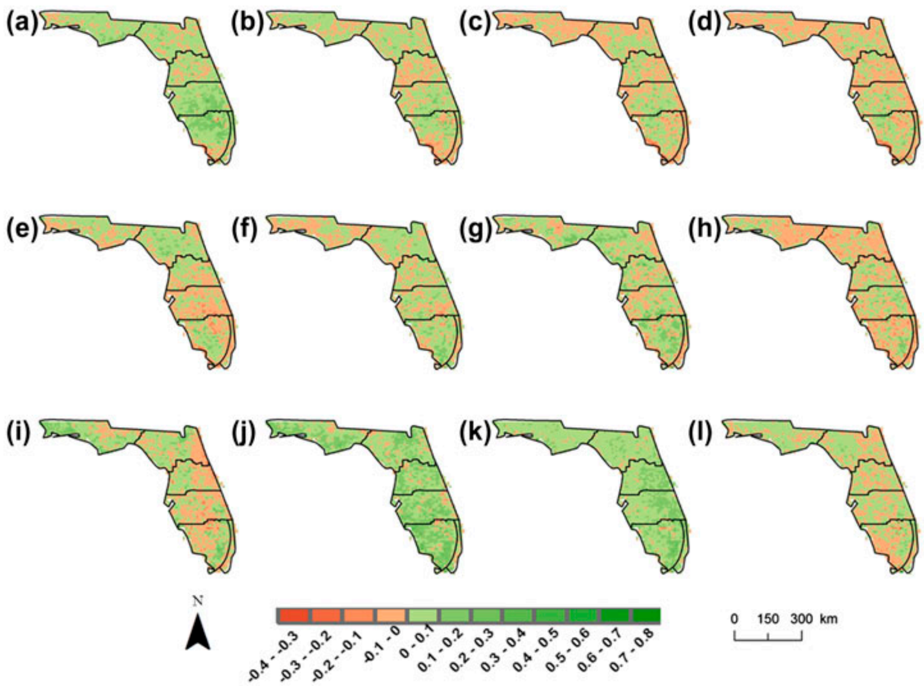

Figure 13. Monthly values of the massive persistence metric, *M*, from (a) January to (l) December for all land uses combined, 1982–2006. Positive scores are shown in green and negative scores are shown in red.

August exhibit less marked, but fairly consistent patterns of declining NDVI, while other summer signals are weak or mixed. Changes are most marked in the northerly climate divisions, which receive a high proportion of their annual precipitation during winter. Given the highly vegetated nature of much of Florida, and precipitation as the main driver of plant growth, this fairly universal change in NDVI might be explained by a low-frequency shift in climatic patterns, such as the increase in winter precipitation in the southeast United States identified by Karl and Knight (1998).

The Atlantic Multidecadal Oscillation (AMO), a series of naturally occurring low-frequency (20–40 years) changes in sea surface temperatures of the North Atlantic Ocean of about 0.5 °C, is a possible driver of this pattern. According to Enfield et al. (2001), warm phases of the AMO are associated with below normal precipitation in most of the United States, and extremes in phases cause the inflow to Lake Okeechobee in south Florida to vary by up to 40%. They conclude that, in general, it is summer precipitation in the United States that is most greatly impacted, however winter precipitation in Florida exhibits significant positive correlations with the AMO (Enfield et al., 2001). Precipitation in central and south Florida is more abundant in warm phases of the AMO and droughts and wildfires are more common in the cool phase. The relationship weakens in north Florida. Secondly, in warm phases of the AMO, the numbers of tropical storms maturing into major hurricanes are greater. During the warm phase from 1944 to 1970, the number of major hurricanes averaged 2.7 annually; during the 1971–1994 cold phase, it was 1.5 (Goldenberg, Landsea, Mestas-Nuñez, & Gray, 2001) and, with the return to warm phase in 1995, the number increased to 3.8 (Curtis, 2008;

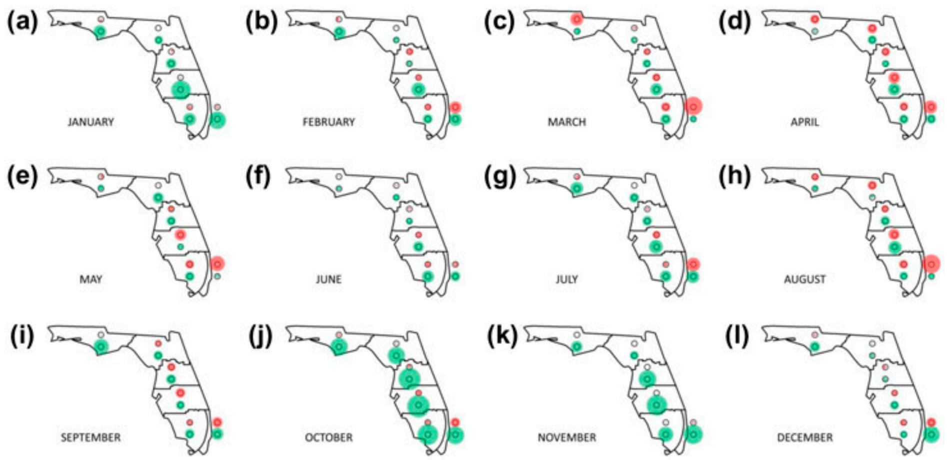

Figure 14. The proportion of significant changes of massive persistence variable, *M*, for developed land for each climate division 1982–2006. The hallow black circle size represents 5% of pixels which falls into each category for each climate division. Significant positive changes are shown in green color and significant negative changes are shown in red color.

Enfield et al., 2001; Goldenberg et al., 2001; Miralles-Wilhelm, Trimble, Podestá, Letson, & Broad, 2005). As a consequence, the warm phase of AMO is associated with fewer drought events over Florida (Mo, Schemm, & Yoo, 2009). Additionally, Curtis (2008) reported increased precipitation intensity (August–October) during the warm phases and Nogueira, Keim, Brown, and Robbins (2013) detected a strong positive correlation between tropical cyclone precipitation (June–November) and AMO. Observations and model simulations (Mo et al., 2009; Tootle & Piechota, 2004)

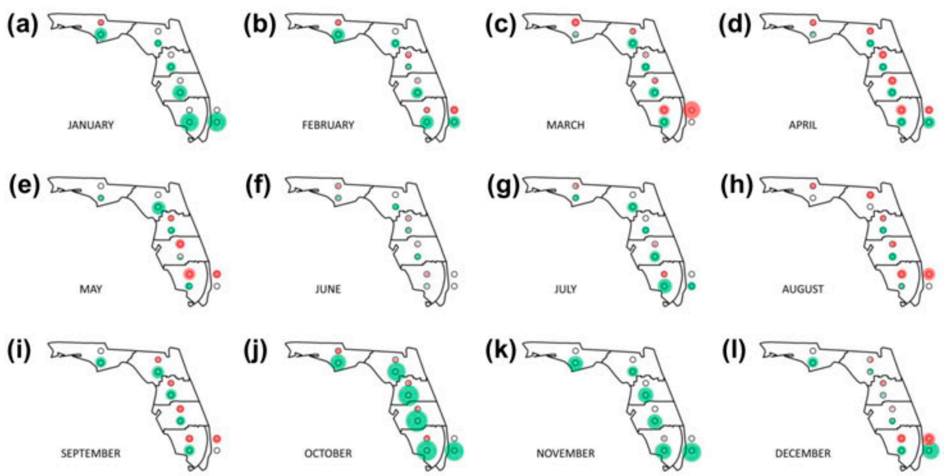

Figure 15. The proportion of significant changes of massive persistence variable, *M*, for agricultural land for each climate division 1982–2006. The hallow black circle size represents 5% of pixels which falls into each category for each climate division. Significant positive changes are shown in green color and significant negative changes are shown in red color.

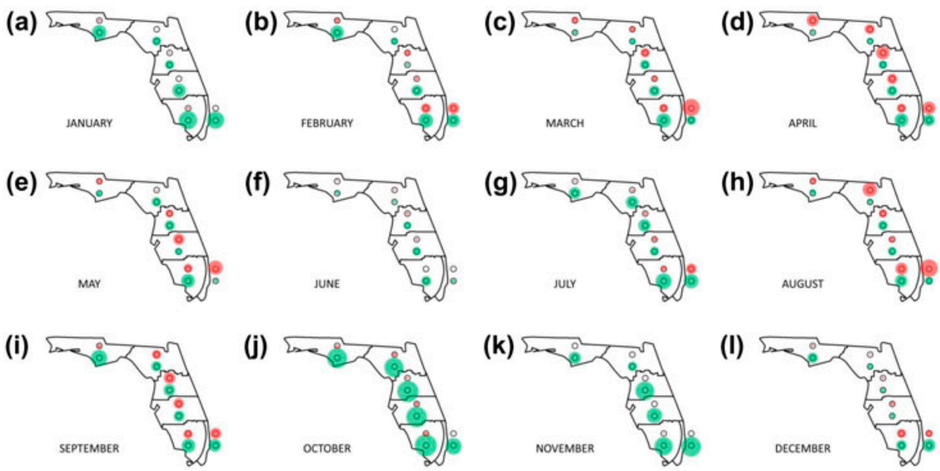

Figure 16. The proportion of significant changes of massive persistence variable, *M*, for palustrine wetlands for each climate division 1982–2006. The hallow black circle size represents 5% of pixels which falls into each category for each climate division. Significant positive changes are shown in green color and significant negative change is shown in red color.

Table 2. Generalized summary of the three monthly metrics of NDVI persistence (*D*, *R*, and *M*) across the six climate divisions in the research. Green indicates a tendency for increased greenness, brown for decreased greenness, and white indicates an indeterminate or mixed signal within the climate division based on the particular metric.

Climate Division	I			II			III			IV			V			VI		
Metric	D	R	M	D	R	M	D	R	M	D	R	M	D	R	M	D	R	M
November	green	green	green	green	green	green	green	green	green	green	green		green		green	green	green	green
December	green		green	green		green	green							green			green	green
January	green	green	green	green		green	green		green	green	green	green	green	green	green	green		green
February	green	green	green	green	green	green	brown	green			green	green	brown			brown		
March	brown	brown	brown	brown	brown		brown				green			green		brown		brown
April	brown	brown	brown							green	green		green					brown
May	green			green	green	green	green			green		brown	green				brown	brown
June				green	green		green	green		green	green		green		green		brown	
July	green		green	green		green	green		green		green	green	green		green			
August	brown		brown	brown	brown	brown			green	brown	green		brown			brown		brown
September		green	green		green		brown	green		brown	green		brown	brown		brown		
October	green	green	green	green	green	green	green		green	green		green	green	green	green	green		green

indicate that the combination of a cold ENSO event in a warm AMO phase amplifies the impact on regional drought. Although uncertainties still exist, both drought and prolonged heavy precipitation are key drivers of vegetation growth and NDVI.

6. Conclusions

The combined use of mean variance analysis and the metrics of persistence permits the objective analysis of monthly remotely sensed time-series data related to the state of vegetation over an extensive and diverse area. Trends of increasing greenness, particularly in the winter, and in the northern parts of the state are in keeping with previously reported impacts of ENSO and AMO on precipitation over Florida. However, precipitation variability alone does not offer a complete picture of drivers of vegetation patterns. Florida's rapid growth in population and associated societal demands during the 20th century have extensively transformed the natural landscape through agriculture, urbanization, and the diversion of surface water features, which may be responsible for more localized conditions and patterns. Identification of such anomalies from the climatic signal illuminates areas in which investigations of local drivers of LULCC are needed. The roles of precipitation and land-cover change will be addressed further in future research but initial results presented here, derived from this time-series based approach, imply linkages between vegetation dynamics and low-frequency climate drivers in addition to more anthropogenic controls. By coupling climate variability and anthropogenic influences, the dynamics of Florida's vegetation becomes more complex and richer for scientific research. Spatial variation across the state was significant, both as a function of climate division and of land cover. While providing a complete overview of vegetation changes over 26 recent years, this research also analyzes the information at a fine temporal and spatial scale for such a time-series-based statewide scale, highlighting statewide impacts of both inter- and intra-annual variability. Understanding of such complex dynamics is key in developing future climate scenarios and impact studies, especially in regions of rapid change such as Florida. This research provides a novel framework and starting point for such future studies.

Acknowledgements

The authors would like to thank Dr Youliang Qiu for his stimulating conversations and great technical assistance in the GIS programming. We also thank Nicholas Campiz for his kind help with the GIS database. The comments, observations and suggestions of two very thorough and positive reviewers improved the quality of the manuscript greatly.

References

Abtew, W., & Trimble, P. (2010). El Niño–Southern Oscillation link to South Florida hydrology and water management applications. *Water Resources Management, 24*, 4255–4271. doi:10.1007/s11269-010-9656-2

Allen Jr., L. H., Boote, K. J., Jones, J. W., Jones, P. H., Valle, R. R., Acock, B., … Dahlman, R. C. (1987). Response of vegetation to rising carbon dioxide: Photosynthesis, biomass, and seed yield of soybean. *Global Biogeochemical Cycles, 1*(1), 1–14. doi:10.1029/GB001i001p00001

Anyamba, A., & Eastman, J. R. (1996). Interannual variability of NDVI over Africa and its relation to El Niño/Southern Oscillation. *International Journal of Remote Sensing, 17*, 2533–2548. doi:10.1080/01431169608949091

Anyamba, A., & Tucker, C. J. (2005). Analysis of Sahelian vegetation dynamics using NOAA-AVHRR NDVI data from 1981–2003. *Journal of Arid Environments, 63*, 596–614.
Azzali, S., & Menenti, M. (2000). Mapping vegetation-soil-climate complexes in southern Africa using temporal Fourier analysis of NOAA-AVHRR NDVI data. *International Journal of Remote Sensing, 21*, 973–996. doi:10.1080/014311600210380
Barbosa, H. A., Huete, A. R., & Baethgen, W. E. (2006). A 20-year study of NDVI variability over the Northeast region of Brazil. *Journal of Arid Environments, 67*, 288–307.
Bartholomé, E., & Belward, A. S. (2005). GLC2000: A new approach to global land cover mapping from earth observation data. *International Journal of Remote Sensing, 26*, 1959–1977.
Baumann, M., Kuemmerle, T., Elbakidze, M., Ozdogan, M., Radeloff, V. C., Keuler, N. S., … Hostert, P. (2011). Patterns and drivers of post-socialist farmland abandonment in Western Ukraine. *Land Use Policy, 28*, 552–562. doi:10.1016/j.landusepol.2010.11.003
Beckage, B., Platt, W. J., Slocum, M. G., & Panko, B. (2003). Influence of the El Niño Southern Oscillation on fire regimes in the Florida Everglades. *Ecology, 84*, 3124–3130.
Bégué, A., Vintrou, E., Ruelland, D., Claden, M., & Dessay, N. (2011). Can a 25-year trend in Soudano-Sahelian vegetation dynamics be interpreted in terms of land use change? A remote sensing approach. *Global Environmental Change, 21*, 413–420.
Bobbink, R., Hornung, M., & Roelofs, J. G. M. (1998). The effects of air-borne nitrogen pollutants on species diversity in natural and semi-natural European vegetation. *Journal of Ecology, 86*, 717–738.
Bonan, G. B., Oleson, K. W., Vertenstein, M., Levis, S., Zeng, X., Dai, Y., … Yang, Z.-L. (2002). The land surface climatology of the community land model coupled to the NCAR community climate model. *Journal of Climate, 15*, 3123–3149. doi:10.1175/1520-0442(2002)015<3123:tlscot>2.0.co;2
Bosch, J. M., & Hewlett, J. D. (1982). A review of catchment experiments to determine the effect of vegetation changes on water yield and evapotranspiration. *Journal of Hydrology, 55*, 3–23. doi:10.1016/0022-1694(82)90117-2
Bounoua, L., DeFries, R., Collatz, G. J., Sellers, P., & Khan, H. (2002). Effects of land cover conversion on surface climate. *Climatic Change, 52*, 29–64.
Brenner, J. (1991). Southern Oscillation anomalies and their relationship to wildfire activity in Florida. *International Journal of Wildland Fire, 1*, 73–78.
Brolley, J. M., O'Brien, J. J., Schoof, J., & Zierden, D. (2007). Experimental drought threat forecast for Florida. *Agricultural and Forest Meteorology, 145*, 84–96. doi:10.1016/j.agrformet.2007.04.003
Cao, M. K., & Woodward, F. I. (1998). Dynamic responses of terrestrial ecosystem carbon cycling to global climate change. *Nature, 393*, 249–252. doi:10.1038/30460
Carlson, T. N., & Ripley, D. A. (1997). On the relation between NDVI, fractional vegetation cover, and leaf area index. *Remote Sensing of Environment, 62*, 241–252. doi:10.1016/s0034-4257(97)00104-1
Chase, T. N., Pielke Sr., R. A., Kittel, T. G. F., Nemani, R. R., & Running, S. W. (2000). Simulated impacts of historical land cover changes on global climate in northern winter. *Climate Dynamics, 16*, 93–105. doi:10.1007/s003820050007
Choudhury, B. J. (1987). Relationships between vegetation indices, radiation absorption, and net photosynthesis evaluated by a sensitivity analysis. *Remote Sensing of Environment, 22*, 209–233. doi:10.1016/0034-4257(87)90059-9
COAPS. (2014). *ENSO index according to JMA SSTA (1868–present)*. Florida State University. Retrieved January 22, 2014, from http://coaps.fsu.edu/jma
Colditz, R. R., Schmidt, M., Conrad, C., Hansen, M. C., & Dech, S. (2011). Land cover classification with coarse spatial resolution data to derive continuous and discrete maps for complex regions. *Remote Sensing of Environment, 115*, 3264–3275. doi:10.1016/j.rse.2011.07.010
Cronin, T. M. (2002). Climate variability from the Florida Bay sedimentary record: Possible teleconnections to ENSO, PNA and CNP. *Climate Research, 19*, 233–245.
Cuo, L., Lettenmaier, D. P., Alberti, M., & Richey, J. E. (2009). Effects of a century of land cover and climate change on the hydrology of the Puget Sound basin. *Hydrological Processes, 23*, 907–933.
Curtis, S. (2008). The Atlantic multidecadal oscillation and extreme daily precipitation over the US and Mexico during the hurricane season. *Climate Dynamics, 30*, 343–351. doi:10.1007/s00382-007-0295-0

de Chazal, J., & Rounsevell, M. D. A. (2009). Land-use and climate change within assessments of biodiversity change: A review. *Global Environmental Change, 19*, 306–315. doi:10.1016/j.gloenvcha.2008.09.007

DeFries, R. (2008). Terrestrial vegetation in the coupled human-earth system: Contributions of remote sensing. *Annual Review of Environment and Resources, 33*, 369–390. doi:10.1146/annurev.environ.33.020107.113339

DeFries, R. S., Field, C. B., Fung, I., Collatz, G. J., & Bounoua, L. (1999). Combining satellite data and biogeochemical models to estimate global effects of human-induced land cover change on carbon emissions and primary productivity. *Global Biogeochemical Cycles, 13*, 803–815.

de Jong, R., de Bruin, S., de Wit, A., Schaepman, M. E., & Dent, D. L. (2011). Analysis of monotonic greening and browning trends from global NDVI time-series. *Remote Sensing of Environment, 115*, 692–702. doi:10.1016/j.rse.2010.10.011

Deser, C., Phillips, A. S., & Hurrell, J. W. (2004). Pacific interdecadal climate variability: Linkages between the tropics and the North Pacific during boreal winter since 1900. *Journal of Climate, 17*, 3109–3124.

Di Gregorio, A., & Jansen, L. J. M. (1998). *Land Cover Classification System (LCCS): Classification concepts and user manual*. Rome: Food and Agriculture Organization of the United Nations.

Drummond, M. A., & Loveland, T. R. (2010). Land-use pressure and a transition to forest-cover loss in the Eastern United States. *BioScience, 60*, 286–298. doi:10.1525/bio.2010.60.4.7

Duncan, B. W., Shao, G., & Adrian, F. W. (2009). Delineating a managed fire regime and exploring its relationship to the natural fire regime in East Central Florida, USA: A remote sensing and GIS approach. *Forest Ecology and Management, 258*, 132–145. doi:10.1016/j.foreco.2009.03.053

Eklundh, L., & Olsson, L. (2003). Vegetation index trends for the African Sahel 1982–1999. *Geophysical Research Letters, 30*, 1430–1433.

Enfield, D. B., Mestas-Nuñez, A. M., & Trimble, P. J. (2001). The Atlantic multidecadal oscillation and its relation to rainfall and river flows in the continental U.S. *Geophysical Research Letters, 28*, 2077–2080. doi:10.1029/2000GL012745

Eugenio, Y. A., Richards, P., Walker, R., & Caldas, M. M. (2011). Statistical confirmation of indirect land use change in the Brazilian Amazon. *Environmental Research Letters, 6*, 024010. doi:10.1088/1748-9326/6/2/024010

Feddema, J. J., Oleson, K. W., Bonan, G. B., Mearns, L. O., Buja, L. E., Meehl, G. A., & Washington, W. M. (2005). The importance of land-cover change in simulating future climates. *Science, 310*, 1674–1678.

Fensholt, R., & Proud, S. R. (2012). Evaluation of earth observation based global long term vegetation trends – Comparing GIMMS and MODIS global NDVI time series. *Remote Sensing of Environment, 119*, 131–147. doi:10.1016/j.rse.2011.12.015

Fensholt, R., Rasmussen, K., Nielsen, T. T., & Mbow, C. (2009). Evaluation of earth observation based long term vegetation trends – Intercomparing NDVI time series trend analysis consistency of Sahel from AVHRR GIMMS, Terra MODIS and SPOT VGT data. *Remote Sensing of Environment, 113*, 1886–1898.

Foley, J. A., DeFries, R., Asner, G. P., Barford, C., Bonan, G., Carpenter, S. R., … Snyder, P. K. (2005). Global consequences of land use. *Science, 309*, 570–574.

Friedl, M. A., Sulla-Menashe, D., Tan, B., Schneider, A., Ramankutty, N., Sibley, A., & Huang, X. (2010). MODIS collection 5 global land cover: Algorithm refinements and characterization of new datasets. *Remote Sensing of Environment, 114*, 168–182.

Fuller, D. O. (1998). Trends in NDVI time series and their relation to rangeland and crop production in Senegal, 1987–1993. *International Journal of Remote Sensing, 19*, 2013–2018. doi:10.1080/014311698215135

Gaiser, E. E., McCormick, P. V., Hagerthey, S. E., & Gottlieb, A. D. (2011). Landscape patterns of periphyton in the Florida Everglades. *Critical Reviews in Environmental Science and Technology, 41*(Suppl. 1), 92–120.

Gao, B.-C. (1996). NDWI – A normalized difference water index for remote sensing of vegetation liquid water from space. *Remote Sensing of Environment, 58*, 257–266.

Gershunov, A. (1998). ENSO influence on intraseasonal extreme rainfall and temperature frequencies in the contiguous United States: Implications for long-range predictability. *Journal of Climate, 11*, 3192–3203. doi:10.1175/1520-0442(1998)011<3192:EIOIER>2.0.CO;2

Gischler, E., Hudson, J., & Storz, D. (2009). Growth of Pleistocene massive corals in south Florida: Low skeletal extension-rates and possible ENSO, decadal, and multi-decadal cyclicities. *Coral Reefs, 28*, 823–830. doi:10.1007/s00338-009-0537-1

Goldenberg, S. B., Landsea, C. W., Mestas-Nuñez, A. M., & Gray, W. M. (2001). The recent increase in Atlantic hurricane activity: Causes and implications. *Science, 293*, 474–479.

Gould, W. (2000). Remote sensing of vegetation, plant species richness, and regional biodiversity hotspots. *Ecological Applications, 10*, 1861–1870. doi:10.1890/1051-0761(2000)010[1861:rsovps]2.0.co;2

Grimm, N. B., Faeth, S. H., Golubiewski, N. E., Redman, C. L., Wu, J., Bai, X., & Briggs, J. M. (2008). Global change and the ecology of cities. *Science, 319*, 756–760.

Gu, L., Post, W. M., Baldocchi, D., Black, T. A., Verma, S. B., Vesala, T., & Wofsy, S. C. (2003). Phenology of vegetation photosynthesis. In M. D. Schwartz (Ed.), *Phenology: An integrative environmental science* (pp. 467–485). The Netherlands: Springer.

Gurgel, H. C., & Ferreira, N. J. (2003). Annual and interannual variability of NDVI in Brazil and its connections with climate. *International Journal of Remote Sensing, 24*, 3595–3609. doi:10.1080/0143116021000053788

Gutman, G., Janetos, A. C., Justice, C. O., Moran, E. F., Mustard, J. F., Rindfuss, R. R., … Cochrane, M. A. (2004). *Land change science: Observing, monitoring and understanding trajectories of change on the earth's surface* (Vol. 1). The Netherlands: Springer.

Gutman, G. G. (1999). On the use of long-term global data of land reflectances and vegetation indices derived from the advanced very high resolution radiometer. *Journal of Geophysical Research, 104*, 6241–6255. doi:10.1029/1998jd200106

Haile, S. G., Nair, V. D., & Nair, P. K. R. (2010). Contribution of trees to carbon storage in soils of silvopastoral systems in Florida, USA. *Global Change Biology, 16*, 427–438.

Hansen, J. W., Hodges, A. W., & Jones, J. W. (1998). ENSO influences on agriculture in the Southeastern United States. *Journal of Climate, 11*, 404–411. doi:10.1175/1520-0442(1998)011<0404:EIOAIT>2.0.CO;2

Hansen, J. W., Jones, J. W., Kiker, C. F., & Hodges, A. W. (1999). El Niño–Southern Oscillation impacts on winter vegetable production in Florida. *Journal of Climate, 12*, 92–102.

Harley, G. L., Grissino-Mayer, H. D., & Horn, S. P. (2012). Fire history and forest structure of an endangered subtropical ecosystem in the Florida Keys, USA. *International Journal of Wildland Fire, 22*, 394–404.

Harrison, M. (2013). Understanding and visualizing and ENSO-based fire climatology in Florida, USA: A case method using cluster analysis. *Southeastern Geographer, 53*, 381–402.

Helldén, U., & Tottrup, C. (2008). Regional desertification: A global synthesis. *Global and Planetary Change, 64*, 169–176.

Henry, J. A., Portier, K. M., & Coyne, J. (1994). *The climate and weather of Florida*. Sarasota, FL: Pineapple Press.

Hill, M. J., & Donald, G. E. (2003). Estimating spatio-temporal patterns of agricultural productivity in fragmented landscapes using AVHRR NDVI time series. *Remote Sensing of Environment, 84*, 367–384. doi:10.1016/S0034-4257(02)00128-1

Hogda, K. A., Karlsen, S. R., & Solheim, I. (2001). *Climatic change impact on growing season in Fennoscandia studied by a time series of NOAA AVHRR NDVI data*. Paper presented at the Geoscience and Remote Sensing Symposium, 2001. IGARSS '01. IEEE 2001 International, Sydney.

Huang, Y. H., Saiers, J. E., Harvey, J. W., Noe, G. B., & Mylon, S. (2008). Advection, dispersion, and filtration of fine particles within emergent vegetation of the Florida Everglades. *Water Resources Research, 44*, W04408.

Immerzeel, W. W., Quiroz, R. A., & de Jong, S. M. (2005). Understanding precipitation patterns and land use interaction in Tibet using harmonic analysis of SPOT VGT-S10 NDVI time series. *International Journal of Remote Sensing, 26*, 2281–2296. doi:10.1080/01431160512331326611

Jacquin, A., Sheeren, D., & Lacombe, J.-P. (2010). Vegetation cover degradation assessment in Madagascar savanna based on trend analysis of MODIS NDVI time series. *International Journal of Applied Earth Observation and Geoinformation, 12*(Suppl. 1), S3–S10. doi:10.1016/j.jag.2009.11.004

Jagtap, S. S., Jones, J. W., Hildebrand, P., Letson, D., O'Brien, J. J., Podestá, G., … Zazueta, F. (2002). Responding to stakeholder's demands for climate information: From research to applications in Florida. *Agricultural Systems, 74*, 415–430. doi:10.1016/S0308-521X(02)00048-3

Jakubauskas, M. E., Legates, D. R., & Kastens, J. H. (2002). Crop identification using harmonic analysis of time-series AVHRR NDVI data. *Computers and Electronics in Agriculture, 37*, 127–139. doi:10.1016/S0168-1699(02)00116-3

Jarlan, L., Tourre, Y., Mougin, E., Philippon, N., & Mazzega, P. (2005). Dominant patterns of AVHRR NDVI interannual variability over the Sahel and linkages with key climate signals (1982–2003). *Geophysical Research Letters, 32*, L04701. doi: 10.1029/2004GL021841

Jeyaseelan, A., Roy, P., & Young, S. (2007). Persistent changes in NDVI between 1982 and 2003 over India using AVHRR GIMMS (Global Inventory Modeling and Mapping Studies) data. *International Journal of Remote Sensing, 28*, 4927–4946.

Jonsson, P., & Eklundh, L. (2002). Seasonality extraction by function fitting to time-series of satellite sensor data. *IEEE Transactions on Geoscience and Remote Sensing, 40*, 1824–1832. doi:10.1109/TGRS.2002.802519

Jordan, C. L. (1984). *Water resources: Atlas of Florida*. Tallahassee (FL): Florida State University.

Kalnay, E., & Cai, M. (2003). Corrigendum: Impact of urbanization and land-use change on climate. *Nature, 425*, 528–531.

Kaplan, S. (2012). Response of urban and non-urban land cover in a semi-arid ecosystem to summer precipitation variability. *Journal of the Arizona-Nevada Academy of Science, 43*, 77–85. doi:10.2181/036.043.0203

Karl, T. R., & Knight, R. W. (1998). Secular trends of precipitation amount, frequency, and intensity in the United States. *Bulletin of the American Meteorological Society, 79*, 231–241.

Keim, B. D., Fischer, M. R., & Wilson, A. M. (2005). Are there spurious precipitation trends in the United States Climate Division database? *Geophysical Research Letters, 32*, L04702. doi:10.1029/2004GL021985

King, A. W., Post, W. M., & Wullschleger, S. D. (1997). The potential response of terrestrial carbon storage to changes in climate and atmospheric CO_2. *Climatic Change, 35*, 199–227. doi:10.1023/a:1005317530770

Lambin, E. F., & Ehrlich, D. (1996). The surface temperature-vegetation index space for land cover and land-cover change analysis. *International Journal of Remote Sensing, 17*, 463–487. doi:10.1080/01431169608949021

Lambin, E. F., & Geist, H. J. (2006). *Land-use and land-cover change*. Berlin: Springer.

Lambin, E. F., & Strahlers, A. H. (1994). Change-vector analysis in multitemporal space: A tool to detect and categorize land-cover change processes using high temporal-resolution satellite data. *Remote Sensing of Environment, 48*, 231–244. doi:10.1016/0034-4257(94)90144-9

Lambin, E. F., Turner, B. L., Geist, H. J., Agbola, S. B., Angelsen, A., Bruce, J. W., … Folke, C. (2001). The causes of land-use and land-cover change: Moving beyond the myths. *Global Environmental Change, 11*, 261–269.

LaRoche, F. B., & Ferriter, A. (1992). The rate of expansion of melaleuca in South Florida. *Journal of Aquatic Plant Management, 30*, 62–65.

Lee, R., Yu, F., Price, K. P., Ellis, J., & Shi, P. (2002). Evaluating vegetation phenological patterns in Inner Mongolia using NDVI time-series analysis. *International Journal of Remote Sensing, 23*, 2505–2512. doi:10.1080/01431160110106087

Li, F., Kustas, W. P., Prueger, J. H., Neale, C. M., & Jackson, T. J. (2005). Utility of remote sensing-based two-source energy balance model under low- and high-vegetation cover conditions. *Journal of Hydrometeorology, 6*, 878–891.

Li, Z., & Kafatos, M. (2000). Interannual variability of vegetation in the United States and its relation to El Niño/Southern Oscillation. *Remote Sensing of Environment, 71*, 239–247. doi:10.1016/s0034-4257(99)00034-6

Los, S. O., Justice, C. O., & Tucker, C. J. (1994). A global 1° by 1° NDVI data set for climate studies derived from the GIMMS continental NDVI data. *International Journal of Remote Sensing, 15*, 3493–3518. doi:10.1080/01431169408954342
Lu, H., Raupach, M. R., McVicar, T. R., & Barrett, D. J. (2003). Decomposition of vegetation cover into woody and herbaceous components using AVHRR NDVI time series. *Remote Sensing of Environment, 86*(1), 1–18.
Markon, C. J., Fleming, M. D., & Binnian, E. F. (1995). Characteristics of vegetation phenology over the Alaskan landscape using AVHRR time-series data. *Polar Record, 31*, 179–190.
Marshall, C. H., Pielke Sr., R. A., Steyaert, L. T., & Willard, D. A. (2004). The impact of anthropogenic land-cover change on the Florida peninsula sea breezes and warm season sensible weather. *Monthly Weather Review, 132*, 28–52.
Martínez, B., & Gilabert, M. A. (2009). Vegetation dynamics from NDVI time series analysis using the wavelet transform. *Remote Sensing of Environment, 113*, 1823–1842. doi:10.1016/j.rse.2009.04.016
Matthews, H. D., Weaver, A. J., Meissner, K. J., Gillett, N. P., & Eby, M. (2004). Natural and anthropogenic climate change: Incorporating historical land cover change, vegetation dynamics and the global carbon cycle. *Climate Dynamics, 22*, 461–479. doi:10.1007/s00382-004-0392-2
McAlpine, C. A., Syktus, J., Ryan, J. G., Deo, R. C., McKeon, G. M., McGowan, H. A., & Phinn, S. R. (2009). A continent under stress: Interactions, feedbacks and risks associated with impact of modified land cover on Australia's climate. *Global Change Biology, 15*, 2206–2223.
McCloy, K. R., Los, S., Lucht, W., & Højsgaard, S. (2005). A comparative analysis of three long-term NDVI datasets derived from AVHRR satellite data. *EARSeL eProceedings, 4*, 52–69.
McGuire, A. D., Melillo, J. M., Joyce, L. A., Kicklighter, D. W., Grace, A. L., Moore III, B., & Vorosmarty, C. J. (1992). Interactions between carbon and nitrogen dynamics in estimating net primary productivity for potential vegetation in North America. *Global Biogeochemical Cycles, 6*, 101–124. doi:10.1029/92gb00219
Meng, M., Ni, J., & Zong, M. (2011). Impacts of changes in climate variability on regional vegetation in China: NDVI-based analysis from 1982 to 2000. *Ecological Research, 26*, 421–428.
Menges, E. S., & Deyrup, M. A. (2001). Postfire survival in south Florida slash pine: Interacting effects of fire intensity, fire season, vegetation, burn size, and bark beetles. *International Journal of Wildland Fire, 10*, 53–63.
Menzel, A. (2000). Trends in phenological phases in Europe between 1951 and 1996. *International Journal of Biometeorology, 44*, 76–81. doi:10.1007/s004840000054
Milesi, C., Samanta, A., Hashimoto, H., Kumar, K. K., Ganguly, S., Thenkabail, P. S., … Myneni, R. B. (2010). Decadal variations in NDVI and food production in India. *Remote Sensing, 2*, 758–776.
Millward, A. A., Piwowar, J. M., & Howarth, P. J. (2006). Time-series analysis of medium-resolution, multisensor satellite data for identifying landscape change. *Photogrammetric Engineering and Remote Sensing, 72*, 653–663.
Miralles-Wilhelm, F., Trimble, P., Podestá, G., Letson, D., & Broad, K. (2005). Climate-based estimation of hydrologic inflow into Lake Okeechobee, Florida. *Journal of Water Resources Planning and Management, 131*, 394–401. doi:10.1061/(ASCE)0733-9496(2005)131:5(394)
Misra, V., & DiNapoli, S. (2012). Understanding the wet season variations over Florida. *Climate Dynamics*, *40,* 1361–1372. doi:10.1007/s00382-012-1382-4
Mo, K. C., Schemm, J.-K. E., & Yoo, S.-H. (2009). Influence of ENSO and the Atlantic multidecadal oscillation on drought over the United States. *Journal of Climate, 22*, 5962–5982.
Myneni, R. B., Keeling, C. D., Tucker, C. J., Asrar, G., & Nemani, R. R. (1997). Increased plant growth in the northern high latitudes from 1981 to 1991. *Nature, 386*, 698–702.
National Research Council. (2005). *Radiative forcing of climate change: Expanding the concept and addressing uncertainties*. Washington, DC: The National Academies Press.
Neeti, N., Rogan, J., Christman, Z., Eastman, J. R., Millones, M., Schneider, L., … Ghimire, B. (2011). Mapping seasonal trends in vegetation using AVHRR-NDVI time series in the Yucatán Peninsula, Mexico. *Remote Sensing Letters, 3*, 433–442. doi:10.1080/01431161.2011.616238

Nogueira, R., Keim, B., Brown, D., & Robbins, K. (2013). Variability of rainfall from tropical cyclones in the eastern USA and its association to the AMO and ENSO. *Theoretical and Applied Climatology, 112*, 273–283. doi:10.1007/s00704-012-0722-y
Obeysekera, J., Irizarry, M., Park, J., Barnes, J., & Dessalegne, T. (2011). Climate change and its implications for water resources management in south Florida. *Stochastic Environmental Research and Risk Assessment, 25*, 495–516. doi:10.1007/s00477-010-0418-8
Olsson, L., Eklundh, L., & Ardö, J. (2005). A recent greening of the Sahel – Trends, patterns and potential causes. *Journal of Arid Environments, 63*, 556–566.
Pettorelli, N., Vik, J. O., Mysterud, A., Gaillard, J.-M., Tucker, C. J., & Stenset, N. C. (2005). Using the satellite-derived NDVI to assess ecological response to environmental change. *Trends in Ecology and Evolution, 20*, 503–510.
Philippon, N., Jarlan, L., Martiny, N., Camberlin, P., & Mougin, E. (2007). Characterization of the interannual and intraseasonal variability of West African vegetation between 1982 and 2002 by means of NOAA AVHRR NDVI data. *Journal of Climate, 20*, 1202–1218.
Pickup, G., & Foran, B. D. (1987). The use of spectral and spatial variability to monitor cover change on inert landscapes. *Remote Sensing of Environment, 23*, 361–363. doi:10.1016/0034-4257(87)90046-0
Porporato, A., Laio, F., Ridolfi, L., & Rodriguez-Iturbe, I. (2001). Plants in water-controlled ecosystems: Active role in hydrologic processes and response to water stress. *Advances in Water Resources, 24*, 725–744. doi:10.1016/s0309-1708(01)00006-9
Raynolds, M. K., Walker, D. A., Epstein, H. E., Pinzon, J. E., & Tucker, C. J. (2012). A new estimate of tundra-biome phytomass from trans-Arctic field data and AVHRR NDVI. *Remote Sensing Letters, 3*, 403–411.
Ricotta, C., Avena, G., & De Palma, A. (1999). Mapping and monitoring net primary productivity with AVHRR NDVI time-series: Statistical equivalence of cumulative vegetation indices. *ISPRS Journal of Photogrammetry and Remote Sensing, 54*, 325–331. doi:10.1016/S0924-2716(99)00028-3
Rindfuss, R. R., Walsh, S. J., Turner, B. L., Fox, J., & Mishra, V. (2004). Developing a science of land change: Challenges and methodological issues. *Proceedings of the National Academy of Sciences, 101*, 13976–13981.
Ropelewski, C. F., & Halpert, M. S. (1986). North American precipitation and temperature patterns associated with the El Niño/Southern Oscillation (ENSO). *Monthly Weather Review, 114*, 2352–2362.
Ross, M. S., Ruiz, P. L., Sah, J. P., & Hanan, E. J. (2009). Chilling damage in a changing climate in coastal landscapes of the subtropical zone: A case study from south Florida. *Global Change Biology, 15*, 1817–1832.
Running, S. W., & Nemani, R. R. (1988). Relating seasonal patterns of the AVHRR vegetation index to simulated photosynthesis and transpiration of forests in different climates. *Remote Sensing of Environment, 24*, 347–367. doi:10.1016/0034-4257(88)90034-x
Sakamoto, T., Yokozawa, M., Toritani, H., Shibayama, M., Ishitsuka, N., & Ohno, H. (2005). A crop phenology detection method using time-series MODIS data. *Remote Sensing of Environment, 96*, 366–374. doi:10.1016/j.rse.2005.03.008
Scanlon, T. M., Albertson, J. D., Caylor, K. K., & Williams, C. A. (2002). Determining land surface fractional cover from NDVI and rainfall time series for a savanna ecosystem. *Remote Sensing of Environment, 82*, 376–388. doi:10.1016/S0034-4257(02)00054-8
Schmidt, N., Lipp, E. K., Rose, J. B., & Luther, M. E. (2001). ENSO influences on seasonal rainfall and river discharge in Florida. *Journal of Climate, 14*, 615–628. doi:10.1175/1520-0442(2001)014<0615:eiosra>2.0.co;2
Schmidt, N., & Luther, M. (2002). ENSO impacts on salinity in Tampa Bay, Florida. *Estuaries, 25*, 976–984. doi:10.1007/bf02691345
Shalaby, A., & Tateishi, R. (2007). Remote sensing and GIS for mapping and monitoring land cover and land-use changes in the Northwestern coastal zone of Egypt. *Applied Geography, 27*, 28–41.
Sitch, S., Smith, B., Prentice, I. C., Arneth, A., Bondeau, A., Cramer, W., … Venevsky, S. (2003). Evaluation of ecosystem dynamics, plant geography and terrestrial carbon cycling in the LPJ dynamic global vegetation model. *Global Change Biology, 9*, 161–185.
Smith, M. J., & Pain, C. F. (2009). Applications of remote sensing in geomorphology. *Progress in Physical Geography, 33*, 568–582.

Southworth, J., Cumming, G. S., Marsik, M., & Binford, M. W. (2006). Linking spatial and temporal variation at multiple scales in a heterogeneous landscape. *The Professional Geographer, 58*, 406–420.

Southworth, J., Munroe, D., & Nagendra, H. (2004). Land cover change and landscape fragmentation – Comparing the utility of continuous and discrete analyses for a western Honduras region. *Agriculture, Ecosystems and Environment, 101*, 185–205. doi:10.1016/j.agee.2003.09.011

Stephenson, N. L. (1990). Climatic control of vegetation distribution: The role of the water balance. *The American Naturalist, 135*, 649–670.

Stow, D. A., Hope, A., McGuire, D., Verbyla, D., Gamon, J., Huemmrich, F., … Tape, K. (2004). Remote sensing of vegetation and land-cover change in Arctic tundra ecosystems. *Remote Sensing of Environment, 89*, 281–308.

Tang, R., Li, Z.-L., & Tang, B. (2010). An application of the T_s–VI triangle method with enhanced edges determination for evapotranspiration estimation from MODIS data in arid and semi-arid regions: Implementation and validation. *Remote Sensing of Environment, 114*, 540–551.

Todd, M. J., Muneepeerakul, R., Pumo, D., Azaele, S., Miralles-Wilhelm, F., Rinaldo, A., & Rodriguez-Iturbe, I. (2010). Hydrological drivers of wetland vegetation community distribution within Everglades National Park, Florida. *Advances in Water Resources, 33*, 1279–1289.

Tootle, G. A., & Piechota, T. C. (2004). Suwannee river long range streamflow forecasts based on seasonal climate predictors. *Journal of the American Water Resources Association, 40*, 523–532.

Townshend, J., Justice, C., Li, W., Gurney, C., & McManus, J. (1991). Global land cover classification by remote sensing: Present capabilities and future possibilities. *Remote Sensing of Environment, 35*, 243–255.

Tucker, C. J., Pinzon, J. E., Brown, M. E., Slayback, D. A., Pak, E. W., Mahoney, R., … El Saleous, N. (2005). An extended AVHRR 8 km NDVI dataset compatible with MODIS and SPOT vegetation NDVI data. *International Journal of Remote Sensing, 26*, 4485–4498. doi:10.1080/01431160500168686

Turner, B. L., Lambin, E. F., & Reenberg, A. (2007). The emergence of land change science for global environmental change and sustainability. *Proceedings of the National Academy of Sciences, 104*, 20666–20671. doi:10.1073/pnas.0704119104

Turner, B. L., Skole, D. L., Sanderson, S., Fischer, G., Fresco, L., & Leemans, R. (1995). *Land-use and land-cover change. Science/research plan*. Stockholm: IGBP Secretariat.

Turner, W., Spector, S., Gardiner, N., Fladeland, M., Sterling, E., & Steininger, M. (2003). Remote sensing for biodiversity science and conservation. *Trends in Ecology and Evolution, 18*, 306–314.

US Census Bureau. (2012). *State and county quickfacts: Florida*. Retrieved from http://quickfacts.census.gov/qfd/states/12000.html

USGCRP. (2009). *Global climate change impacts in the United States*. Retrieved from http://nca2009.globalchange.gov/southeast

Vedwan, N., Ahmad, S., Miralles-Wilhelm, F., Broad, K., Letson, D., & Podesta, G. (2008). Institutional evolution in Lake Okeechobee management in Florida: Characteristics, impacts, and limitations. *Water Resources Management, 22*, 699–718. doi:10.1007/s11269-007-9187-7

Veldkamp, A., & Lambin, E. F. (2001). Predicting land-use change. *Agriculture, Ecosystems and Environment, 85*(1–3), 1–6. doi:10.1016/S0167-8809(01)00199-2

Verbesselt, J., Hyndman, R., Newnham, G., & Culvenor, D. (2010). Detecting trend and seasonal changes in satellite image time series. *Remote Sensing of Environment, 114*, 106–115. doi:10.1016/j.rse.2009.08.014

Wang, Q., Tenhunen, J., Dinh, N. Q., Reichstein, M., Vesala, T., & Keronen, P. (2004). Similarities in ground- and satellite-based NDVI time series and their relationship to physiological activity of a Scots pine forest in Finland. *Remote Sensing of Environment, 93*, 225–237. doi:10.1016/j.rse.2004.07.006

Wardlow, B. D., & Egbert, S. L. (2008). Large-area crop mapping using time-series MODIS 250 m NDVI data: An assessment for the U.S. Central Great Plains. *Remote Sensing of Environment, 112*, 1096–1116. doi:10.1016/j.rse.2007.07.019

Warner, T. A., & Campagna, D. J. (2009). *Remote sensing with IDRISI Taiga: A beginner's guide*. Hong Kong: Geocarto International Centre.

Washington-Allen, R. A., Ramsey, R. D., West, N. E., & Norton, B. E. (2008). Quantification of the ecological resilience of drylands using digital remote sensing. *Ecology and Society, 13* (1).

Washington-Allen, R. A., West, N. E., & Ramsey, R. D. (2003, July). *Remote sensing-based dynamical systems analysis of sagebrush steppe vegetation in rangelands*. Paper presented at the Proceedings of the VII International Rangelands Congress in Durban, South Africa.

Waylen, P. R., Southworth, J., Gibbes, C., & Tsai, H. (in press). Time series analysis of land cover change: Developing statistical tools to determine significance of land cover changes in persistence analyses. *Remote Sensing*.

Weng, Q. (2002). Land use change analysis in the Zhujiang Delta of China using satellite remote sensing, GIS and stochastic modelling. *Journal of Environmental Management, 64*, 273–284. doi:10.1006/jema.2001.0509

Wessels, K. J., Prince, S. D., Frost, P. E., & van Zyl, D. (2004). Assessing the effects of human-induced land degradation in the former homelands of northern South Africa with a 1 km AVHRR NDVI time-series. *Remote Sensing of Environment, 91*, 47–67. doi:10.1016/j.rse.2004.02.005

White, M. A., & Nemani, R. R. (2006). Real-time monitoring and short-term forecasting of land surface phenology. *Remote Sensing of Environment, 104*, 43–49.

Wilson, A., & Kirkby, M. (1980). *Mathematics for geographers and planners*. Oxford: Clarendon Press.

Wilson, M. F., & Henderson-Sellers, A. (1985). A global archive of land cover and soils data for use in general circulation climate models. *Journal of Climatology, 5*, 119–143.

Wu, A., Hsieh, W. W., & Shabbar, A. (2005). The nonlinear patterns of North American winter temperature and precipitation associated with ENSO. *Journal of Climate, 18*, 1736–1752.

Wu, B., Zhou, T., & Li, T. (2009). Contrast of rainfall–SST relationships in the western North Pacific between the ENSO-developing and ENSO-decaying summers. *Journal of Climate, 22*, 4398–4405.

Xiao, J., Shen, Y., Ge, J., Tateishi, R., Tang, C., Liang, Y., & Huang, Z. (2006). Evaluating urban expansion and land use change in Shijiazhuang, China, by using GIS and remote sensing. *Landscape and Urban Planning, 75*, 69–80.

Zhou, Q., Li, B., & Kurban, A. (2008). Trajectory analysis of land cover change in arid environment of China. *International Journal of Remote Sensing, 29*, 1093–1107.

Zimmermann, N. E., Washington-Allen, R. A., Ramsey, R. D., Schaepman, M. E., Mathys, L., Kötz, B., … Edwards, T. C. (2007). Modern remote sensing for environmental monitoring of landscape state and trajectories. *Landscape Series, 8*, 65–91. doi:10.1007/978-1-4020-4436-6_6

Zorn, M. R., & Waylen, P. R. (1997). Seasonal response of mean monthly streamflow to El Niño/Southern Oscillation in North Central Florida. *The Professional Geographer, 49*, 51–62.